Master of Science thesis in meteorology

UNCERTAINTY IN FOREST-ATMOSPHERE EXCHANGE OF ENERGY AND CARBON DIOXIDE BASED ON TWO VERTICALLY DISPLACED EDDY COVARIANCE SET-UPS

Lauri Heiskanen

18.5.2017

Supervisors:
Prof. Timo Vesala, Dos. Ivan Mammarella, Dos. Üllar Rannik,
Dr. Pasi Kolari, Dr. Olli Peltola

Examiners:
Prof. Timo Vesala, Dos. Ivan Mammarella

UNIVERSITY OF HELSINKI
DEPARTMENT OF PHYSICS

POB 64 (Gustaf Hällströmin katu 2)
00014 University of Helsinki

HELSINGIN YLIOPISTO – HELSINGFORS UNIVERSITET – UNIVERSITY OF HELSINKI

Tiedekunta/Osasto – Fakultet/Sektion – Faculty/Section	Laitos – Institution – Department
Matemaattis-luonnontieteellinen tiedekunta	Fysiikan laitos

Tekijä – Författare – Author
Lauri Heiskanen

Työn nimi – Arbetets titel – Title
Pyörrekovarianssimenetelmällä mitattujen mäntymetsän ja ilmakehän välisen hiilidioksidi- sekä energiavoiden epävarmuustekijät

Oppiaine – Läroämne – Subject
Meteorologia

Työn laji – Arbetets art – Level	Aika – Datum – Month and year	Sivumäärä – Sidoantal – Number of pages
Pro gradu -tutkielma	18.5.2017	50

Tiivistelmä – Referat – Abstract

Tässä Pro gradu -tutkielmassa tutkitaan pyörrekovarianssimenetelmällä mitattujen suomalaisen mäntymetsän ja ilmakehän välisen hiilidioksidin, vesihöyryn sekä havaittavan lämmön voita, ja pyritään selvittämään mittauksiin liittyvien virhelähteiden suuruudet. Voihin liittyvien virheiden suuruutta analysoidaan vertailemalla saman mittaustornin kahdelta eri korkeudelta saatuja mittaustuloksia. Analyysissa pyritään identifioimaan mikäli tuloksissa havaittavat eroavaisuudet aiheutuvat mikrometeorologisista ja biologisista muuttujista vai turbulenttisten virtausten kaoottisuudesta johtuvista mittausvirheistä. Pyörrekovarianssimenetelmän virhelähteet ovat osana aktiivista tieteellistä keskustelua, jossa pyritään parantamaan meteorologisia mittausmenetelmiä.

Tutkimus tehtiin käyttämällä meteorologista aineistoa sekä vuoaineistoa, joka on kerätty Hyytiälän SMEAR II -metsäntutkimusasemalla vuonna 2015. Mittaukset tehtiin 23,3 m sekä 33,0 m korkeudella maanpinnasta. Vuoaineistoa tarkastellaan aina päivittäisestä vaihtelusta koko vuoden kestävään kumulatiiviseen analyysiin. Aineistolle tehdään myös sekä meteorologisiin muuttujiin että kasvillisuusjakaumaan perustuva tarkastelu.

Tutkimuksessa havaittiin mittauskorkeuksien välisen kumulatiivisten hiilidioksidivoiden eron suuruudeksi 49 $\mathrm{gC\ m^{-2}}$ vuodessa (17 % erotus). Kokonaishaihdunnan kumulatiivisen eron arvioidaan olevan 105 mm vuodessa (29 % erotus). Havaittavan lämmön voissa ei ilmennyt merkittävää eroa mittauskorkeuksien välillä.

Hiilidioksidivuossa tai havaittavan lämmön vuossa ei havaita merkittävää eroa, joka aiheutuisi käytettävistä mittauskorkeuksista. Kuitenkin latentin lämmön vuossa ero on havaittavissa, sillä 33,0 m mittaustulokset ovat jatkuvasti pienempiä kuin 23,3 m vastaavat tulokset.

Avainsanat – Nyckelord – Keywords
Pyörrekovarianssi, pohjoinen havumetsä, hiilidioksidivuo, latentin lämmön vuo, havaittavan lämmön vuo, footprint analyysi

Säilytyspaikka – Förvaringställe – Where deposited
Kumpulan tiedekirjasto

Muita tietoja – Övriga uppgifter – Additional information

HELSINGIN YLIOPISTO – HELSINGFORS UNIVERSITET – UNIVERSITY OF HELSINKI

Tiedekunta/Osasto – Fakultet/Sektion – Faculty/Section	Laitos – Institution – Department	
Faculty of Science	Department of Physics	
Tekijä – Författare – Author		
Lauri Heiskanen		
Työn nimi – Arbetets titel – Title		
Uncertainty in forest-atmosphere exchange of energy and carbon dioxide based on two vertically displaced eddy covariance set-ups		
Oppiaine – Läroämne – Subject		
Meteorology		
Työn laji – Arbetets art – Level	Aika – Datum – Month and year	Sivumäärä – Sidoantal – Number of pages
Master's thesis	18.5.2017	50

Tiivistelmä – Referat – Abstract

This thesis is a study of the uncertainties related to the eddy covariance measurement technique on a forest ecosystem that is located in Hyytiälä, Southern Finland. The aim of this study is to analyze carbon dioxide and energy fluxes measured at two vertically displaced eddy covariance set-ups. In particular, to determine if the observed deviations between the set-ups could be linked with micrometeorological or biological variations or if they are resulted just by the stochastic nature of turbulence. The magnitude of uncertainties linked to eddy covariance technique are still under discussion and this thesis attempts to shed a light on these questions.

The analysis is done to half hourly mean flux and meteorological data that was measured at the Hyytiälä SMEAR II –site in 2015 at the heights of 23.3 m and 33.0 m. Monthly, diurnal and cumulative variations of the fluxes are analyzed. A footprint model is used to analyze the flux correlation with the underlying vegetation. The flux dependence on atmospheric stability is also determined.

The analysis shows that the annual cumulative difference of net ecosystem exchange (CO_2 exchange) between the two measurement heights is estimated to be 49 $gC\ m^{-2}year^{-1}$ (17 % difference). The annual cumulative evapotranspiration difference is estimated to be 105 mm (29 % difference). There are no significant differences between the sensible heat fluxes.

The difference between the measurement heights does not seem to influence significantly the flux estimations made with the eddy covariance method. However, the measurement results for latent heat flux acquired from the 33.0 m set-up are continuously smaller than those of the 23.3 m set-up.

Avainsanat – Nyckelord – Keywords

Eddy covariance, boreal forest, carbon dioxide flux, latent heat flux, sensible heat flux, flux footprint

Säilytyspaikka – Förvaringställe – Where deposited

Kumpula Science Library

Muita tietoja – Övriga uppgifter – Additional information

CONTENTS

1 INTRODUCTION

Reliable data collection of the micrometeorological and biological processes is crucial in mitigating the effects of the climate change. Accurate measurement records of the carbon sources and sinks in different ecosystems aids us to understand the repercussions of the human-induced greenhouse gas emissions. The improvements in micrometeorological measurement technology in the last decades has enabled us to have continuous measurements from the rapid fluctuations to interannual variability of the meteorological variables (Baldocchi, 2003). The eddy covariance (EC) method is able to meet the needed requirements of reliable data collection and is utilized in many meteorological measurements.

The eddy covariance technique is widely used and approved measurement method that gives valuable estimates of the ecosystem-atmosphere exchange of greenhouse gasses and energy fluxes (Aubinet et al. 2012). The EC technique is able to measure the ecosystem-atmosphere fluxes from the turbulent motion of air. However, the level of uncertainty of the measurement results is still under discussion and studied. While utilizing the EC method, some assumptions and simplifications must be made, which may cause uncertainties to the results.

If the underlying theoretical assumptions of the EC method are not fully met at the measurement site, the EC method itself creates some systematical uncertainty to the results. To tackle this problem, the requirements are always taken into serious consideration during the measurement site assembly. The ecosystem should be homogeneous, which includes flat topography and uniform roughness elements (Aubinet et al. 2012). However, many sites, like the measurement station analyzed in this thesis, do not have complete homogeneity in all directions. For instance, forests and their canopies are not completely homogeneous surfaces neither in terms of gas exchange nor topography. Other uncertainties related to the theoretical assumptions are thought to be caused by inaccurate nighttime flux measurements as the emissions escape through other transport routes closer to the ground, while never reaching the measurement height (Aubinet et al., 2000).

Random errors in flux estimations emerge from the stochastic nature of turbulence, sampling limitations and the post-processing methods. Then there are the errors caused by the uncertainties due to the instrument system, which are easier to fix as

the measurement technology advances. The stochastic nature of turbulence can cause large random errors while using EC methods. This phenomenon is most visible when the time scales are short, for example in the half-hourly records in CO_2 exchange, as the natural variability of turbulent flux is 10 – 20 % (Wesely and Hart, 1985). Even though the random errors may be large in the individual integrated half hour values, they do diminish to ±5 % in the long term when considering annual values (Goulden et al. 1996).

The carbon balance between the atmosphere and the ecosystem is determined by the carbon dioxide (and methane) surface fluxes. This balance is called net ecosystem exchange (NEE) and for boreal forests the annual NEE values have an approximate magnitude from $-150\ gC\ m^{-2}year^{-1}$ to $-300\ gC\ m^{-2}year^{-1}$, depending on the ecosystem (Aubinet et al. 2000). Richardson et al. (2006) estimated that annual uncertainty of NEE caused by random errors in measurements is $\pm 20\ gC\ m^{-2}year^{-1}$, and Moffat et al. (2007) estimated that the accumulated random error caused by gap filling is about the same magnitude. The total uncertainty of long term EC measurements for NEE are estimated to be about 50 $gC\ m^{-2}year^{-1}$ for measurements at nearly ideal sites (Baldocchi, 2003). The scale of these random errors indicate that the EC method gives passable estimates of the interannual variability in NEE, which are more precise than estimates done by upscaling chamber measurements.

The aim of this thesis is to compare micrometeorological data from two measurement points, both of them with similar characteristics as they represent the same ecosystem, and to find out if the differences are linked to meteorological or biological processes. The Station for Measuring Forest Ecosystem-Atmosphere Relations (SMEAR II) field measurement station is located in Hyytiälä, Southern Finland, where the eddy covariance (EC) measurements of ecosystem exchange are made at two different heights above a Scots pine forest. The measurement set-ups are on the same measurement tower at the heights of 23.3 m and 33.0 m. The dominant tree height is 18 m at the time of making these measurements in 2015.

The main interest is in determining carbon dioxide (CO_2), latent heat (LE), and sensible heat (SH) fluxes of the ecosystem, and based on these measurements to further determine how well the two measurement set-ups describe the underlying

ecosystem. The footprint is the surface area that the flux is considered to represent, which is dependent on the atmospheric stability, the measurement height and the roughness of the surface elements. During unstable (stable) conditions most of the flux originates from the part of the ecosystem that is closer (further away) to the measurement set-up. As a result of the set-ups being located at two different heights, the upper one covers a slightly greater area further away from the tower. This dissimilarity raises the question of whether both of the set-ups still represent the Scots pine forest during all atmospheric stability conditions. Therefore, a footprint model is used to determine if the flux differences could arise from the vegetation distribution, as the pine forest changes to spruce forest in the south.

Assumptions about ecosystem homogeneity cannot be done without knowing the possible impacts of surface and/or weather characteristics. The two measurement set-ups have differing footprint source areas, and thus any heterogeneities in the surface cover may affect the flux measurement results. These heterogeneities might cause directional variations in flux measurements affecting e.g. annual carbon budget estimates. The wind sector analysis reveals if there is any dependence between wind patterns and acquired flux data. The footprint source area distribution is therefore connected to the site-specific weather and wind patterns, but as the footprint analysis in this study is done only in one specific direction the wind patterns can be ignored in the footprint analysis.

Hyytiälä's SMEAR II measurement station is currently in the process of applying for an ICOS-label and one of the aims of this study is to clarify some aspects of the 33.0 m measurement set-up regarding the Integrated Carbon Observation System (ICOS). ICOS is a European Research Infrastructure for quantifying and understanding greenhouse gas balance.

2 THEORY

2.1 Atmospheric boundary layer

Earth's atmosphere is in constant motion. The energy behind this motion is received from the sun's radiation, and as the radiation is not evenly spread across the planet it creates air flows that seek to level out the difference in energy. Energy gradients

create high and low pressure systems in the atmosphere that, in turn with the Coriolis-effect, cause geostrophic winds. These phenomena are mainly observed in the troposphere, which is the lowest of the main atmospheric layers, reaching heights from over 9000 meters at the poles to 17 kilometers at the equator.

The atmosphere near the surface of the earth is divided into different layers depending on which forces dominate the flow of air. These forces are tendency, advection, pressure gradient force, the Coriolis force, the turbulent stress and the molecular stress. In the free atmosphere, the surface has no effect on the flow characteristics, causing the lower limit of this layer to be 1000 meters or more above the ground. The lack of surface friction allows the flow to be in near-geostrophic balance. The layer close to the ground under the free atmosphere is the atmospheric boundary layer (ABL) in which surface friction has significant effect on the flow. The height of ABL varies usually from few hundred meters to over 1000 meters, depending on the atmospheric stability. In the atmospheric boundary layer turbulence is the primary phenomenon that vertically transfers energy, momentum and matter. The atmospheric boundary layer is often divided into two regions after Sutton's model (1953): Ekman layer and inertial surface layer.

The inertial surface layer is a region that extends less than 100 meters above ground. The vertical shearing stress is approximately constant in this layer, and the flow is not affected by the earth's rotation. The wind structure is therefore determined primarily by surface friction and the vertical temperature gradient, which creates a well-mixed turbulent layer. The vertical turbulent fluxes are assumed to be constant with height in the inertial surface layer, which is essential for the ecosystem exchange measurements.

In addition to the two aforementioned layers, there is a turbulent sublayer beneath them, called the roughness sublayer, reaching a height that is about three times the roughness element height. The roughness sublayer is important especially when measurements are made in or just above the canopy – this is because the canopy affects air flow over and in it. In addition, water vapor and carbon dioxide flux sources and sinks, among other features, are greatly affected by the biology and vertical distribution of the foliage.

Directly on the surface there is a laminar boundary layer about a few millimeters thick, where matter and energy are exchanged by molecular movement from higher concentrations to lower ones.

2.1.1 Atmospheric turbulence

The main phenomenon that causes turbulence is the effect of surface friction on the mean wind, where the air flow slows down unevenly due to the roughness of the surface. This causes wind shears to develop, which form turbulent eddies. On an occasion where air flow is deflected by an obstacle, turbulent wakes form adjacent and behind the obstacle. Another source of turbulent motion is in the heating of ground that is caused by the sun's radiative forcing. As the sun's shortwave radiation warms up the ground, the ground conducts and radiates the heat to the air molecules just above it, thus warming the air. This creates a vertical density difference as the warmer air close to the ground expands. This can be derived from the ideal gas law, which air obeys quite well despite being a mixture of several gases;

$$p = R\rho T \tag{2.1}$$

where p is pressure, R is ideal gas constant, ρ is density and T is temperature.

The air parcel close to the ground is less dense than the air above it after heating up, thus rising upwards to a level where the air parcel's physical properties are in equilibrium with the surrounding atmosphere. The rising air causes turbulent eddies to form, and with the wind shear induced eddies they create a well-mixed layer of air close to the ground, as the system tries to reach thermodynamical and chemical equilibrium. This turbulent movement of air transports energy, momentum and chemical compounds vertically. The turbulent vortices behave randomly in all three dimensions.

In stable (unstable) atmosphere the ABL height is lower (higher) and there is less (more) turbulence. Atmospheric stability is a measure of how much available energy there is in the system that can be released as work. In a stable atmosphere, there is negligible surface heating and vertical motion is reduced. Instances when surface heating is absent are typically during nights and especially during winter nights. In a

neutral boundary layer air parcels that are displaced up or down adiabatically maintain exactly the same density as the surrounding air.

2.1.2 Diurnal cycle

The atmospheric boundary layer has a distinct diurnal cycle as the amount of insolation varies between daytime and nighttime (Fig 2.1). As the sun rises, a convective layer forms near the ground by the mechanism described previously (Sect. 2.1.1). This convective layer grows simultaneously with the increase of solar radiation until it hits a peak height of typically 1 km to 2 km by midafternoon. When the sun sets and the air cools close to the ground, the boundary layer collapses as the energy input that maintained turbulence withers away. The rapid cooling of air near to the ground caused by radiative heat loss creates inversion layers as the potential temperature drops. In an inversion layer the air closer to the surface is denser than air above it. The height of inversion grows during the evening until it reaches a height of 100 m to 200 m by midnight. This switches the system from an unstable state to a stable state.

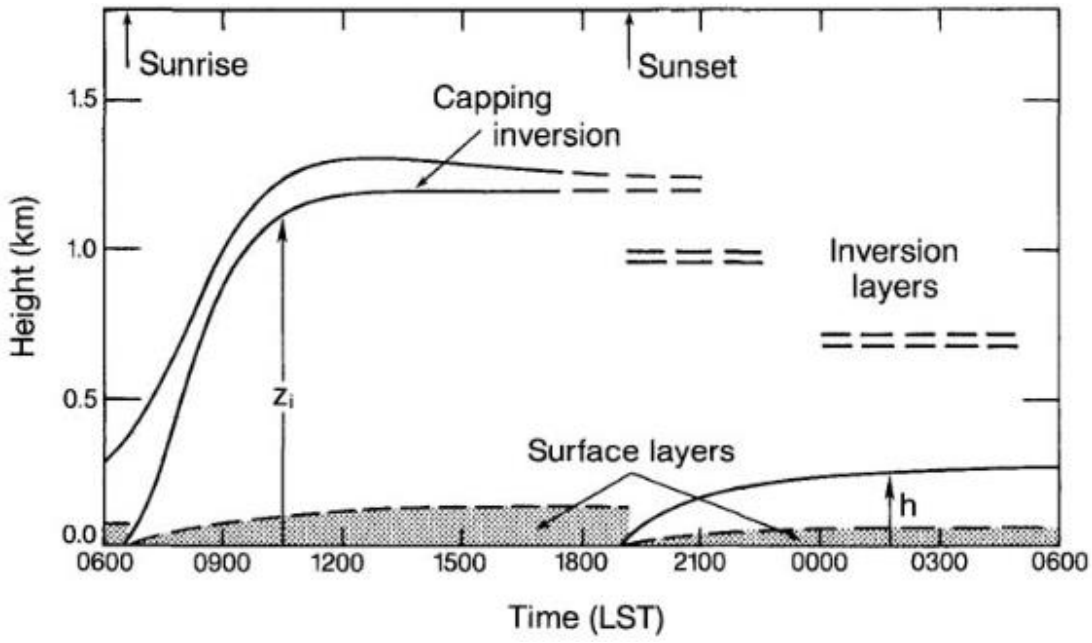

Fig. 2.1 Diurnal ABL. z_i is the daytime maximum height of boundary layer, and h is the nighttime height of the boundary layer. The time indicated is Local Standard Time (LST). (Kaimal et al. 1994)

2.2 Vertical turbulent transport in the surface layer

2.2.1 Reynolds decomposition

Due to the chaotic nature of turbulent motion, measuring the turbulent flow is done with the help of statistical analysis. The flow is separated into mean flow and a fluctuating part of the flow (Fig. 2.2). This is done in all three perpendicular directions; x, y, z. The method is called Reynolds decomposition after Osborne Reynolds who proposed it in 1895.

In Reynolds decomposition time-series of a variable is decomposed into a time-mean part and a fluctuating part.

$$\zeta = \bar{\zeta} + \zeta' \tag{2.2}$$

where

$$\bar{\zeta} = \frac{1}{T}\int_{t}^{t+T} \zeta(t)dt \tag{2.3}$$

where T is the length of the time period and t is a moment in time.

Reynolds postulates determine the averaging rules for the turbulent fluctuations ζ'.

$$I \quad \bar{\zeta}' = 0 \tag{2.4}$$

$$II \quad \overline{\zeta\xi} = \bar{\zeta}\bar{\xi} + \overline{\zeta'\xi'} \tag{2.5}$$

$$III \quad \overline{\bar{\zeta}\xi} = \bar{\zeta}\bar{\xi} \tag{2.6}$$

$$IV \quad \overline{a\zeta} = a\bar{\zeta} \tag{2.7}$$

$$V \quad \overline{\zeta + \xi} = \bar{\zeta} + \bar{\xi} \tag{2.8}$$

where ξ is another variable and a is constant.

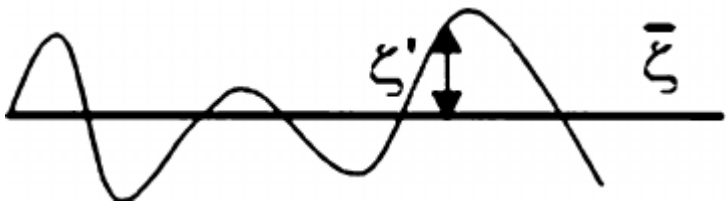

Fig. 2.2 Schematic presentation of Reynolds decomposition of the value ζ (Foken 2008).

2.2.2 Surface fluxes

The main goal when measuring fluxes is to determine the surface exchange of a substance and/or energy. The typical situation that creates vertical fluxes of a substance is when there is a vertical concentration gradient of the substance (e.g. CO_2 or H_2O) with a constant horizontal air flow and vertical mixing of air. This means that the mean vertical wind speed remains zero, but the vertical fluctuations allow the transport of substances from higher concentration levels to lower ones. When the concentration is higher in upward flow than in downward flow, an upward eddy flux emerges.

The flux measurement technique utilizes the assumption that matter and energy are conserved in the system and that the only exchange of matter and energy occurs in a vertical direction between the surface and atmosphere.

The conservation equation of a scalar is:

$$\rho_d \frac{\partial \chi_s}{\partial t} + \rho_d u \frac{\partial \chi_s}{\partial x} + \rho_d v \frac{\partial \chi_s}{\partial y} + \rho_d w \frac{\partial \chi_s}{\partial z} = S_s + D \qquad (2.9)$$

where χ_s is the mixing ratio of one atmospheric component, ρ_d is the dry air density, u, v and w are the wind velocity components, respectively, in the direction of the mean wind x, the lateral wind y and the vertical wind z. S_s is the source/sink term and D is molecular diffusion term. By applying the Reynolds decomposition (Sect. 2.2.1), integrating along the vertical z-axis and assuming there is no horizontal eddy flux divergence, equation 2.9 can be written as:

$$\int_0^{h_m} S_s dz = \overline{\rho_d}\overline{w'\chi'_s} + \int_0^{h_m} \overline{\rho_d} \frac{\partial \overline{\chi_s}}{\partial t} dz + \int_0^{h_m} \overline{\rho_d u} \frac{\partial \overline{\chi_s}}{\partial x} dz + \int_0^{h_m} \overline{\rho_d w} \frac{\partial \overline{\chi_s}}{\partial z} dz \qquad (2.10)$$

I II III IV V

Term I represents the scalar source/sink term which corresponds to the net ecosystem exchange (NEE) when the scalar is CO_2, and to ecosystem evapotranspiration (E) when the scalar is water vapor. Term II represents the vertical turbulent flux at height h_m. The eddy covariance method is the most commonly used method to estimate the term II. The other terms (III-V) are reduced to naught, when the atmospheric stationarity and horizontal homogeneity are met, which means that the vertical turbulent flux measured at h_m is equivalent to the source/sink term. However, in

forest systems, these conditions are not always met, which causes us to utilize the terms III-V.

Term III represents the storage of the scalar below the measurement height. The storage of CO_2 is typically small during the day and on windy nights, as the turbulent motion is mixing the air effectively. On the other hand, during nighttime the mixing conditions can often be poor, which causes substances to accumulate in the surface layer under the measurement height. For example, the nighttime ecosystem respiration of CO_2 causes a notable storage term that must be taken into consideration when estimating the CO_2 flux. If the substances that were stored under the canopy are not present in the morning, but have been flushed further away from the set-up, the measured flux might be underestimated. Therefore, the storage term is crucial while estimating the real flux.

Terms IV and V represent the fluxes by horizontal and vertical advection. If the terrain is not homogeneous but heterogeneous and sloping, an estimation of the term IV is needed. However, horizontal gradients of a scalar are difficult to measure accurately, and therefore measurement sites are allocated to a surface that is as homogeneous as possible. Horizontal gradients of a scalar can be seen for example over sloping terrain, where the nighttime ecosystem respiration of CO_2 flows downhill, while being heavier than air. The vertical advection is typically negligible over low vegetation, but this is not always the case over tall vegetation. Lee (1998) showed that the vertical advection over tall forest canopies is not negligible and could even be more important than turbulent transport during stable nights. With a typical eddy covariance measurement set-up that has limited horizontal resolution, estimating of advection terms is nearly impossible. The last term V is cancelled out as the vertical velocity component (w) and therefore also the vertical advection term is forced to be zero in the equations by a z-coordinate rotation.

2.3 Eddy covariance method

Vertical turbulent fluxes within the atmospheric boundary layer are nowadays usually measured with the eddy covariance measurement method. The eddy covariance method works well when the underlaying surface is assumed to be homogeneous. Homogeneous surface is considered to be flat, horizontal and uniform

when it comes to its roughness elements. The sinks and sources of the measured gasses should also have a homogeneous distribution. The flux measurements should not be affected by the measurement height if the measurements are done at all times inside the ABL, even during the stable nighttime conditions when the height of the ABL is reduced. The roughness elements (e.g. vegetation) should have a homogeneous distribution so that the flow can be considered similar from all wind directions. These definitions allow us to make calculations of vertical 2-dimensional fluxes with the eddy covariance method.

The eddy covariance flux measurements are based on determining the correlation between changes in vertical wind velocity and deviations in a scalar quantity such as mixing ratio of a trace gas or temperature. The measurements must be done in a high enough frequency to capture the variability due to the atmospheric turbulence, which is typically ≤10 Hz depending on the measurement height.

The fluxes measured with the EC technique are momentum flux ($\tau, kg\ m^{-1}\ s^{-1}$), carbon dioxide flux ($F_{CO_2}, \mu mol\ m^{-2}\ s^{-1}$), sensible heat flux ($SH,\ Wm^{-2}$) and latent heat flux ($LE,\ Wm^{-2}$). Other than for momentum flux, upward fluxes are defined as positive.

$$\tau = -\rho_d \overline{w'u'} \tag{2.11}$$

$$F_{CO_2} = \frac{\rho_d}{M_a} \overline{w'\chi'_{CO_2}} \tag{2.12}$$

$$LE = \rho_d L_v \frac{M_w}{M_a} \overline{w'\chi'_{H_2O}} \tag{2.13}$$

$$SH = \rho_d c_p \overline{w'T'} \tag{2.14}$$

where ρ_d is the dry air density, M_a and M_w are the molar masses of dry air and water, L_v is the latent heat of vaporization for water. u' and w' are the turbulent values of horizontal and vertical wind speeds, respectively. χ'_{CO_2} and χ'_{H_2O} are the turbulent values of dry mole fractions of CO_2 and H_2O. T' is the turbulent value of air temperature.

The net ecosystem exchange is determined to be the measured carbon flux (F_{CO_2}) with the change in storage term during the majority of the time period. However, when the atmospheric conditions are not suitable for EC measurements, i.e. during

low turbulence conditions, the friction velocity (u_*) filtering (see Sect. 3.3.1) creates gaps to the data. In the case of missing data, NEE is calculated from modelled gross primary productivity and total ecosystem exchange (see Eq. 2.20). Heat fluxes are calculated as presented in Eq. 2.13 and 2.14 Friction velocity is calculated from the connection to the momentum flux (see Eq. 2.16) using the turbulent wind speed fluctuations and the stability parameter is calculated by using the Obukhov length (see Eq. 2.18)

2.3.1 Friction velocity and stability parameter

The downward flux of momentum (τ) is composed of vectors τ_x and τ_y in their respective directions, but because the flow is assumed to be horizontally homogeneous, the mean wind speed can be assumed to vary only in the vertical direction. This allows us to align the x direction with the wind direction, and as a result $\tau_x = \tau_0$ and $\tau_y = 0$. The wind stress τ_0 on the ground can now be expressed as

$$\tau_o = \rho u_*^2 \tag{2.15}$$

where u_* is the friction velocity.

Friction velocity can also be determined from its relation with the momentum flux in its covariance form:

$$u_*^2 = \left|\overline{u'w'}\right| \tag{2.16}$$

A. M. Obukhov derived a stability parameter in 1946 to tackle the problem of non-neutral conditions, while working on the Monin-Obukhov similarity theory. The often used stability parameter for the surface layer is:

$$\zeta = \frac{z-d}{L} \tag{2.17}$$

where L is the Obukhov length, z is the height above ground and d is the zero-plane displacement height. The variable d is dependent on the canopy characteristics, e.g. for forests d is usually $^2/_3$ or $^3/_4$ of the canopy height.

The Obukhov length is proportional to the height above ground at which production and loss of turbulence are equal during stable atmospheric conditions. It can be estimated by

$$L = -\frac{u_*^3}{k\frac{g}{T}\frac{H}{\rho c_p}} \tag{2.18}$$

where g is acceleration due to the gravity, k is the von Karman constant, which is empirically defined as ~ 0.4, and H is the sensible heat flux. When $L < 0$ the surface layer is statically unstable, and when $L > 0$ the surface layer is statically stable. The surface layer is closer to neutral conditions when the absolute magnitude of Obukhov length is large (or absolute value of $1/L$ is small).

2.4 Footprint

Eddy covariance method gives us a good estimation of the surface-atmosphere exchanges, but the corresponding surface area for the fluxes is dependent on atmospheric stability. The footprint models are used to pinpoint this specific area. The footprint depends on measurement height, surface roughness and atmospheric stability. The flux footprint defines an area influencing the flux measured at a specific measurement location. Footprint is not a discrete area, but an influence function the orientation of which varies depending on wind direction. During stable (unstable) conditions the source/sink area is larger (smaller) due to the differences in turbulent transport. The vertical transport time/distance of particles is shorter during unstable conditions, placing the footprint peak closer to the measurement set-up.

Fetch is the outreach of a homogeneous area that the measurement station is surrounded by. The fetch area should be larger than the footprint area during the most stable conditions. However, not all sites are homogeneous enough in all directions from the measurement tower to meet these criteria. If there are surface inhomogeneities inside the footprint, it is important to know their position and the magnitude of impact on the measured signal.

Functions describing the relationship between the spatial distribution of surface sources/sinks and a signal are called the footprint function. The fundamental definition of the footprint function ϕ is given by the integral equation of diffusion (Wilson and Swaters 1991).

$$\eta = \int_{\mathbb{R}} \phi(\vec{x}, \vec{x}') Q(\vec{x}')\, d\vec{x}' \tag{2.19}$$

where η is the vertical eddy flux being measured at location $\vec{x}$ (which is a vector) and $Q(\vec{x}')$ is the source emission rate/sink strength in the surface-vegetation volume $\mathbb{R}$. ϕ is the flux footprint function.

Mathematically, the surface area of influence on the entire flux goes to infinity and therefore the source area must be restricted to some percentage level of the footprint. Usually these percentage levels are 50 %, 75 % and, as in this study 90 %.

2.5 Flux partitioning

The net ecosystem exchange of CO_2 (NEE) results from two larger fluxes that have opposite signs. Gross primary productivity (GPP) represents the ecosystem uptake of CO_2 due to photosynthesis and the release of CO_2 is called total ecosystem respiration (TER).

$$NEE = -GPP + TER \tag{2.20}$$

Fluxes from atmosphere to biosphere are defined as negative following the usual meteorological convention.

The partitioning of observed NEE into two variables GPP and TER is done to get a grip on the processes causing the carbon flux. This partitioning can be done based on the notion that GPP is virtually zero during nighttime, therefore allowing the estimation of TER straight from the NEE values. However during daytime the partitioning is done using models, and therefore the estimation process is not as straightforward (Aubinet et. al. 2012). This creates uncertainties to the GPP and TER estimations, as the daytime respiration is extrapolated from the nighttime measurements for example with temperature or light response functions.

3 MATERIALS AND METHODS

3.1 Site info

The measurement site at the SMEAR II station is located in Hyytiälä, Southern Finland (61°51´N, 24°17´E, 160 – 180 m a.s.l.), and the two measurement set-ups are on a tall tower at heights of 23.3 m and 33.0 m above ground level and roughly 5 m

and 15 m above the forest canopy. The tower is located at the highest spot in the area (181 m a.s.l.). In 1962 the area was regenerated by clear-cutting and sowing Scots pine seeds. The ecosystem that the SMEAR II station is surrounded by is a typical boreal forest, which is dominantly Scots pine with some spruce and birch patches further away from the measurement tower (Fig 3.1). A notable spruce forest patch is located some 180 meters south of the tower. There are also some small clear-cuts done by the forestry department. The forest is growing on mineral soils that are mainly podzols, but peat soil can also be found in small depressions.

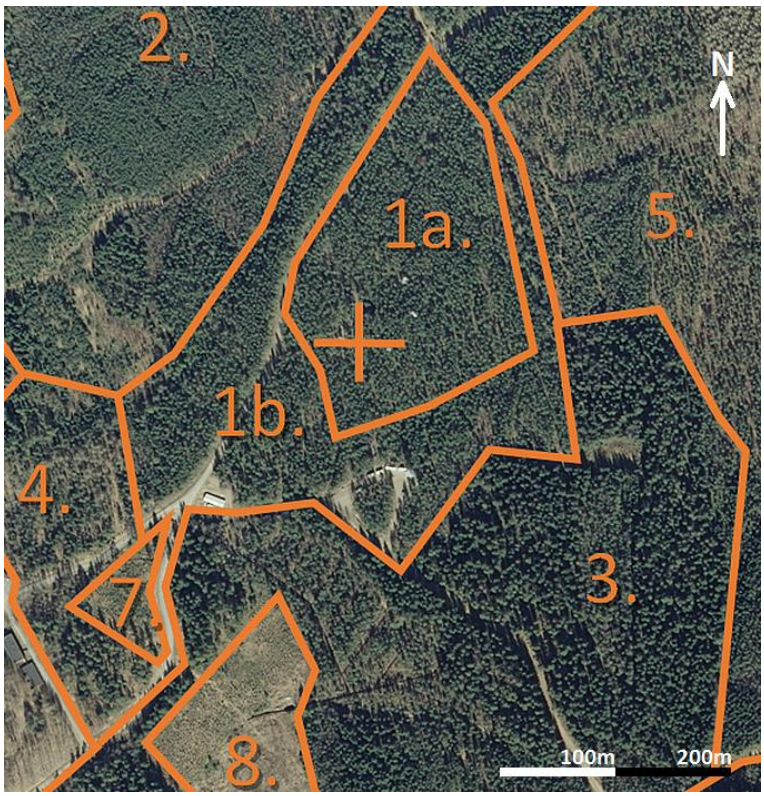

Fig. 3.1 Vegetation map. The cross indicates the tower location. 1a., 1b., 2. and 5. are pine-dominated coniferous stands, 1a. and 1b. form the primary research stand. 3. is spruce-dominated coniferous stands. 4. and 7. are mixed pine and spruce stands and 8. is clear-cut done in 2008.

3.2 Measurement set-up

The eddy covariance measurement technique utilizes high frequency fluctuations in vertical wind velocity and deviations in a scalar quantity. To achieve reliable estimations of surface fluxes a sonic anemometer is used to measure the wind velocity and a gas analyzer to measure the variations in the scalar quantity.

The basic principle of sonic anemometry-thermometry is to measure the difference in a transit time for an ultrasound pulse between sensors. The three sensor pairs are arranged so that they capture the movement of air in all x, y, z directions. The transit time is dependent on the speed of sound in air and wind velocity. Speed of sound is a function of air density, which is determined by the air temperature and the mixing ratio of water vapor.

The second instrument needed to determine CO_2 and water vapor fluxes is a fast-response gas analyzer. The set-ups use closed-path nondispersive infrared (IR) absorption analyzers (commonly referred to as infrared gas analyzer – IRGA), which measure turbulent fluctuations in CO_2 and H_2O molar concentrations at ≤10 Hz. There are open-path analyzers as well, but they are not used in this study. The measurement system has a broadband IR light source, band-pass filters to select according wavelength at which CO_2 and H_2O molecules are absorbed, and a detector. The internal sample cell of a closed-path analyzer is flushed by sampled air, and the reduced intensity of observed light correlates with the molar concentrations of the analyzed gas. A reference signal is used to determine the accurate variations of the detector signal. In the closed-path analyzer, the reference signal is measured using a second cell, which uses a small flow of air with known (in this case zero) CO_2 and H_2O molar concentration.

The anemometers that were used in this study are both from Gill Instruments Ltd. (Lymington, Hampshire, England). For the 23.3 m measurement set-up the ultrasonic anemometer model is Solent Research 1012 R2, and for the 33.0 m set-up a Gill HS-50 ultrasonic anemometer measures wind speeds. The sonic anemometers also measure air temperature.

Both measurement set-ups use gas analyzers provided by Li-Cor Inc. (Lincoln, NE, USA), the model for 23.3 m set-up is LI-6262 and for 33.0 m set-up LI-7200. These closed-path infrared gas analyzers measure CO_2 and H_2O concentrations at high frequencies. The 33.0 m gas analyzer uses a sampling frequency of 10 Hz. For the 23.3 m set-up the signals are digitized and recorded at 21 Hz, but the logging software reduces the sampling frequency to half of that with averaging. Therefore the raw data used to calculate fluxes have a sampling frequency of $\frac{21}{2}$ Hz $\approx$ 10 Hz.

The sample line lengths for the 23.3 m and 33.0 m gas analyzers are 7 m and 0.77 m, respectively. The inside diameters of the sample lines are 4 mm for 23.3 m and 5.3 mm for 33.0 m. Both sample lines are heated with a power of about 5 Wm^{-1} to prevent any condensation of water vapor inside the tubes. The flow rate inside the 23.3 m sample line is 6.1 $L\,min^{-1}$ and inside the 33.0 m sample line 10 $L\,min^{-1}$.

These trace gas flux instruments are typical of those used in most EC flux systems that measure ecosystem exchange of heat, CO_2 and H_2O. The micrometeorological fluxes of CO_2, LE and SH are calculated as 30 min average covariances between the scalars and vertical wind speed using the widely approved flux calculations (Eq. 2.12 – 2.14).

3.3 Data post-processing

The data has to be post processed before it can be analyzed to meet the desired quality criteria. Detrending of the raw data is done with block-averaging. The raw data is despiked using a method that calculates the difference between subsequent data points. Spectral corrections to CO_2 and H_2O fluxes include both low and high frequency signal attenuation. The spectral corrections are performed using a site specific model cospectrum (Mammarella et al., 2009). u_* filtering and gap filling are applied to the data that was used in this study. After the corrections and implementing standard quality criteria the data is ready to be analyzed.

3.3.1 Friction velocity filtering

Filtering methods are applied when the atmospheric conditions are not favorable to eddy covariance measurements. These conditions are met as the turbulence decreases to a level where it is no longer guaranteed that enough of the trace gases are reaching the measurement set-up. During these advection conditions, it is probable that the measurements are underestimating the flux exchange of the ecosystem. The advection problem is most notable when the surface has a slope or other heterogeneities to the characteristics. One way to overcome the advection problem is to apply friction velocity (u_*) filtering.

The friction velocity range is where the EC flux measurements are considered reliable is determined by the nighttime NEE dependence on u_*. The lower u_* filtering threshold value is where the NEE flux values reach a plateau-average. The threshold value for u_* filtering should be as small as possible so that the filtering does not remove copious amounts of data and large enough so that it does not induce a systematic bias into the cumulative values. The u_* threshold varies typically between 0.1 – 0.5 m/s depending on the site-specific characteristics. The characteristics that have an effect on the u_* threshold are the possible heterogeneities in topography, surface roughness and source distribution. The u_* filtering is done to the data studied here with a value of 0.3 m/s.

During stable atmospheric conditions the CO_2 that is stored in the canopy air space may be removed by advection, but if it remains at the site, the gas concentration will be captured by the EC system as the turbulence kicks in (Papale et al. 2006). A storage term is used to take into account the advection problem when the CO_2 is flushed away. The CO_2 fluxes discussed in this study are corrected for storage below the measurement height.

3.3.2 Gap filling

The eddy covariance technique collects data continuously with high temporal resolution. In an ideal set-up there will not be any long gaps in the measurements, but usually there are unavoidable data gaps either related to the measurement set-up or the post-processing methods. These post-processing induced gaps are caused by quality filtering, as some of the measurements are discarded due to non-ideal conditions for the EC method.

Usually the measurement related gaps occur during power breaks, which is particularly common if the measurement set-up is powered with solar panels. Gaps can also be caused by instrument malfunction or regular maintenance work performed at the site. While the gaps related to physical setbacks to measurements may last even for days, data gaps caused by post processing are usually much shorter, but more frequent.

Gap filling is needed when calculating aggregate values, as the daily averages and annual budgets require a full set of data covering the whole timespan. If the data gaps were perfectly randomly distributed, the gap filling could be done simply by taking average of all available data. However, data gaps caused by power failure occur mainly during winter and nighttime due to the use of solar panels, and in post processing u_* filtering removes mainly nighttime data. The data gaps should be filled with data that is representative of the missing period's vegetation status and meteorological conditions. This is true in particular when the ecosystem and its carbon balance is prone to seasonal changes, as with the boreal forest studied here.

4 RESULTS

This study uses eddy covariance data and other standard meteorological data collected at the SMEAR II station during the year 2015 at the heights of 23.3 m and 33.0 m. The data was post-processed and ready to be analyzed. The analyzed meteorological data is averaged to 30 min means from the raw 10 Hz measurement data. Monthly, diurnal and cumulative variations of the fluxes are analyzed. A footprint model is used to analyze the flux correlation with the underlying vegetation. The flux dependence on atmospheric stability and wind direction is also determined. The meteorological variables that are analyzed in this study are shown in Table 4.1.

Symbol	Unit	Variable
CO_2 flux		
NEE	$\mu mol\ m^{-2}s^{-1}$	Net Ecosystem Exchange
GPP	$\mu mol\ m^{-2}s^{-1}$	Gross Primary Productivity
TER	$\mu mol\ m^{-2}s^{-1}$	Total Ecosystem Respiration
Heat flux		
LE	$W\ m^{-2}$	Latent heat flux
SH	$W\ m^{-2}$	Sensible heat flux
Shear stress		
u^*	$m\ s^{-1}$	Friction velocity
Stability		
$1/L$	m^{-1}	Obukhov length

Table 4.1 The meteorological variables analyzed in this study

4.1 Monthly variation

The data is split between daytime and nighttime for monthly values by the definition that during day the solar angle is $> 0°$ and during night it is $< -3°$. This leaves a small part of the data unused, but it is done to make sure that no photosynthesis is observed in the nighttime data. The monthly mean values are calculated from the half hourly post processed data (Sect. 3.2). The difference between the two measurement set-ups for every month is calculated from those mean values.

The monthly mean NEE values (Fig. 4.1) vary from 0.5 $\mu mol\, m^{-2}s^{-1}$ during winter to $-6\, \mu mol\, m^{-2}s^{-1}$ during summer, with the largest carbon uptake values in August. This pattern follows the general ecosystem activity of a boreal forest. The absolute difference of monthly NEE between the two measurement heights is less than 0.6 $\mu mol\, m^{-2}s^{-1}$, which means that the relative difference does not exceed 20 % during summer. The mean daytime NEE values at 23.3 m are slightly smaller during wintertime and slightly larger during rest of the year. But if we think about NEE in absolute values, the 33.0 m values are slightly larger during the whole year. The 33.0 m observations show that winter respiration (positive NEE) is larger than the 23.3 m respiration, and the results are similar with uptake (negative NEE) during the growing season.

Mean daytime GPP values (Fig. 4.2) for 33.0 m are larger virtually for the entire year 2015. Note that NEE partitioning uses –GPP (Sect. 2.6). The monthly mean GPP values between $0.5 - 14\, \mu mol\, m^{-2}s^{-1}$. The absolute difference in the monthly mean values is largest during growing season in summer, but the difference remains percentage-wise almost constant during the whole year. The absolute difference varies between $0 - 2\, \mu mol\, m^{-2}s^{-1}$, and the relative difference hovers around 20 %.

Mean nighttime TER values (Fig. 4.3) for 33.0 m are larger for the whole year. TER behaves similarly to the GPP, meaning that the largest absolute difference can be seen during summer and early autumn. The monthly mean values of TER are smaller, $0.5 - 7\, \mu mol\, m^{-2}s^{-1}$, than those of GPP, indicating that the forest ecosystem acts as a carbon sink. The absolute difference of TER 23.3 m and 33.0 m varies between $0 - 1.5\, \mu mol\, m^{-2}s^{-1}$, and the relative difference hovers aroud 20 %.

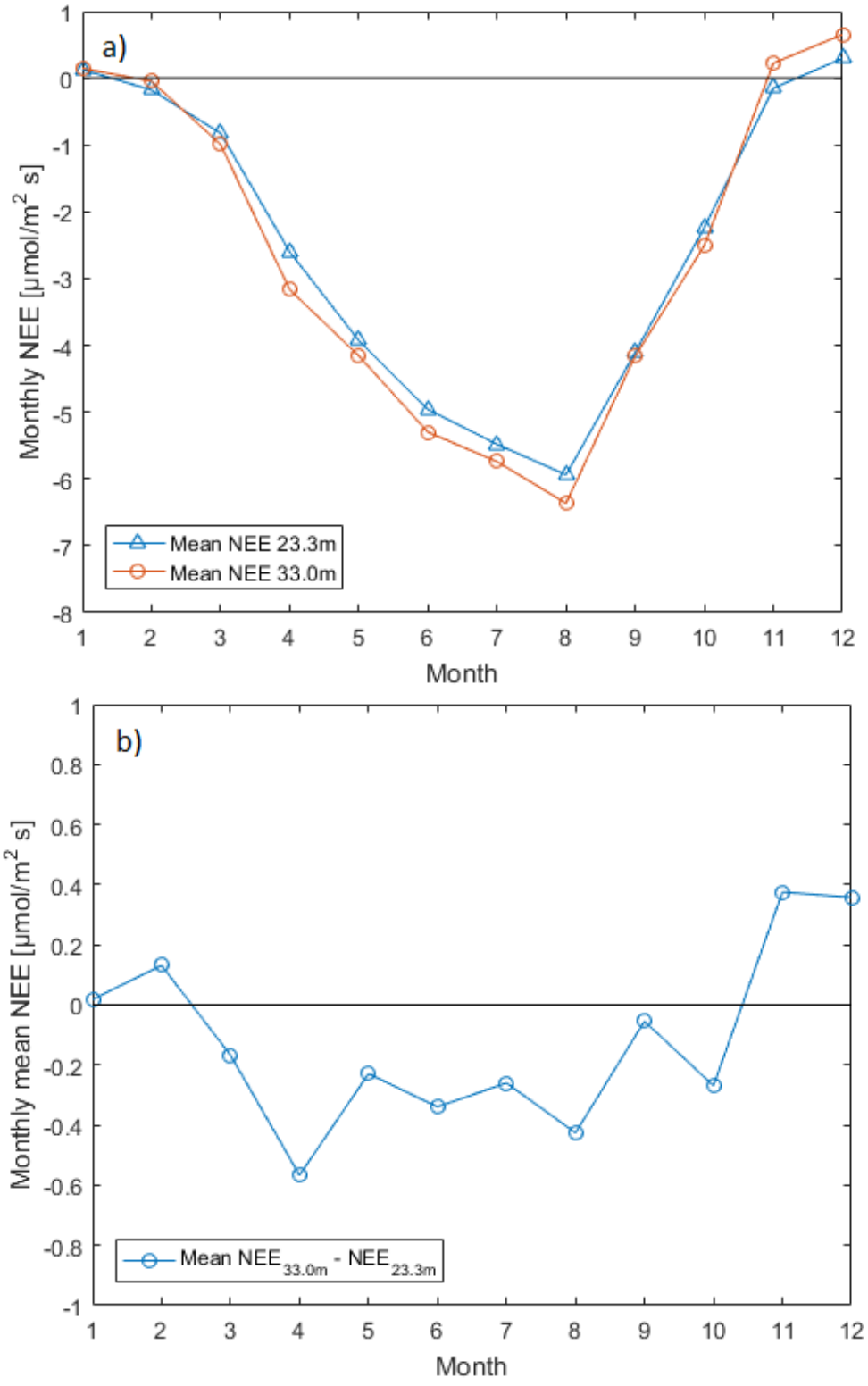

Fig. 4.1 Monthly mean daytime NEE in 2015 measured at 23.3 m and 33.0 m heights (a). Difference in monthly mean daytime NEE values between the measurement set-ups (b).

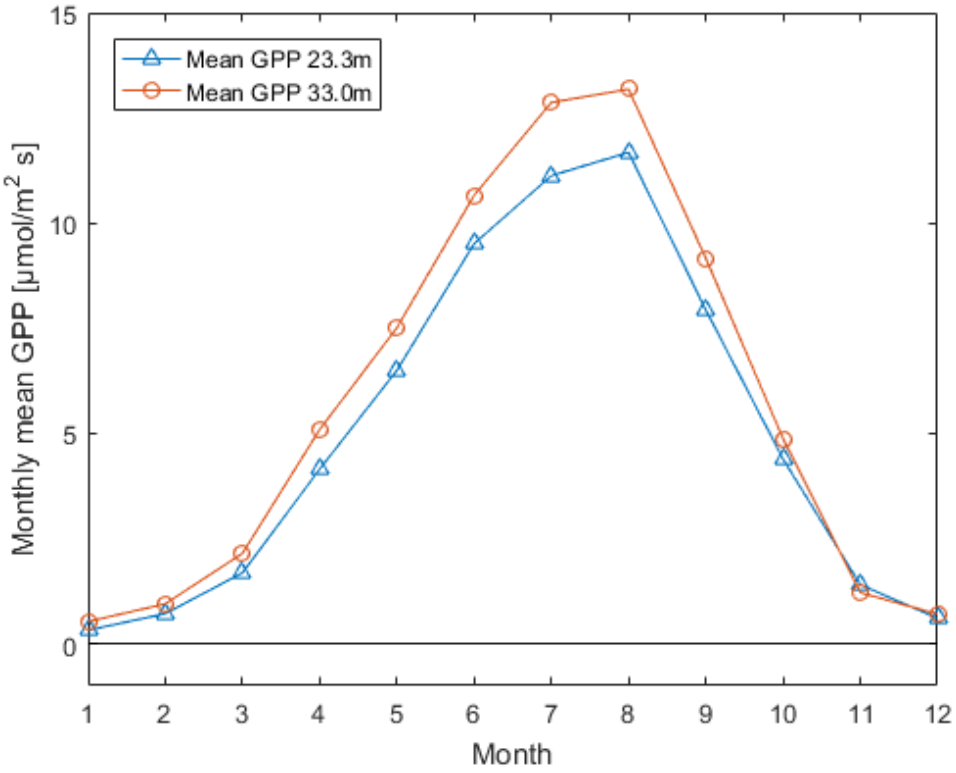

Fig. 4.2 Monthly mean daytime gross primary productivity in 2015 at 23.3 m and 33.0 m. Note that the flux partitioning (Eq. 2.22) uses -GPP.

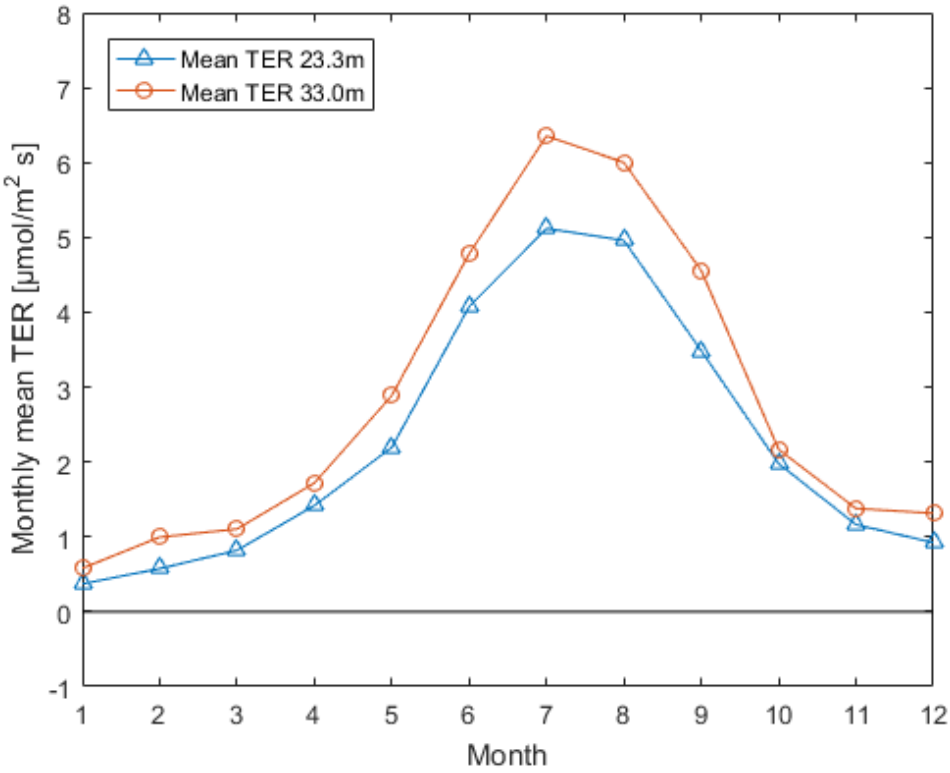

Fig. 4.3 Monthly mean nighttime total ecosystem respiration in 2015 at 23.3 m and 33.0 m.

The daytime monthly mean LE values (Fig. 4.4) are larger during summertime, as is expected, since larger amounts of insolation causes more evaporation. LE at 23.3 m remains larger during the whole year, with values ranging from $10\,Wm^{-2}$ to $95\,Wm^{-2}$. Meanwhile LE at 33.0 m measures lower values of $-5\,Wm^{-2}$ to $90\,Wm^{-2}$. The negative values during November and December are quite peculiar, as it would indicate condensation of water, which rarely occurs during cold and dry conditions. The absolute and relative differences in LE is most substantial during winter, reaching up to $15\,Wm^{-2}$/ 80 %. The difference during summer is only $\sim 3\,Wm^{-2}$/ 5 %. The 23.3 m measurements follow the commonly observed pattern of LE in a boreal ecosystem.

Monthly mean nighttime LE for 23.3 m and 33.0 m (Fig. 4.5) showcase the problems with the 33.0 m negative values. The 23.3 m measurements oscillate between $-2 - 10\,Wm^{-2}$. The 33.0 m measured nighttime values of LE stay below the 23.3 m ones throughout the whole year, being mostly negative $2 - (-13)\,Wm^{-2}$. The absolute difference between the measurement set-ups displays 33.0 m mean values that are $4 - 15\,Wm^{-2}$ smaller than the corresponding values of 23.3 m. The annual pattern of nighttime LE is similar in both data sets, but the 33.0 m values stay consistently below the 23.3 m ones, with the greatest difference in November and December.

The daytime mean SH fluxes for every month in 2015 is presented in Fig. 4.6 The SH flux reacts directly to the amount of insolation, and therefore the monthly values are also dependent on the amount of cloud cover. This effect can be seen in June and July, where the SH values drop compared to typical values. Surface temperatures in June and July 2015 were 1.5 – 2.0 °C colder than the 30 year averages (Finnish Meteorological Institute).

Both measurement set-ups record an early SH peak in May at $80\,Wm^{-2}$, while the lowest values are acquired during December, $-30\,Wm^{-2}$ and $-20\,Wm^{-2}$ for 23.3 m and 33.0 m respectively. Negative values show that the amount of outgoing radiation is larger than the amount of insolation. The difference between the set-ups is negligible during summer and remains quite small ($< 15\,Wm^{-2}$) during the rest of the year.

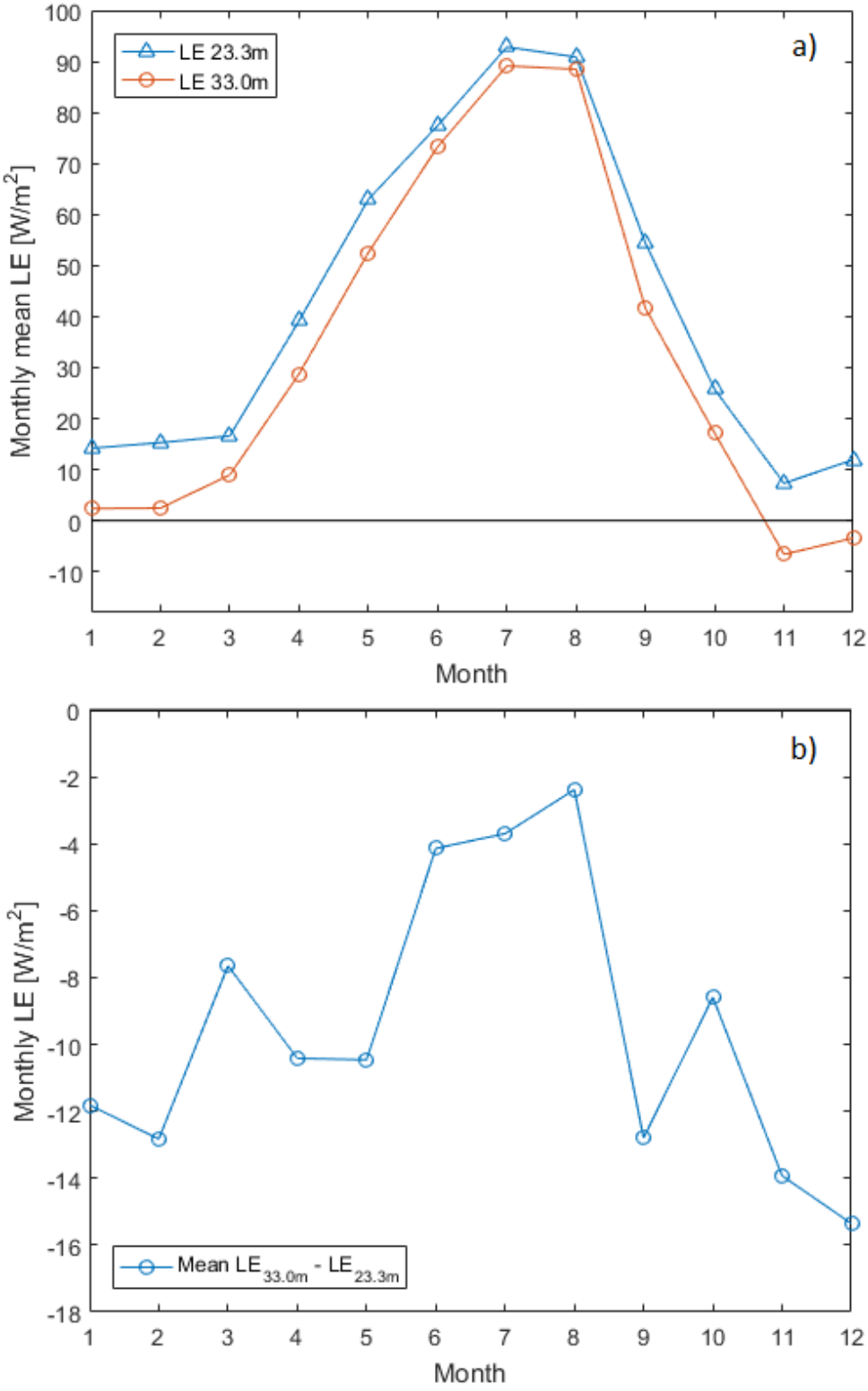

Fig. 4.4 Monthly mean daytime LE flux in 2015 measured at 23.3 m and 33.0 m (a). Monthly mean daytime LE difference between the heights (b).

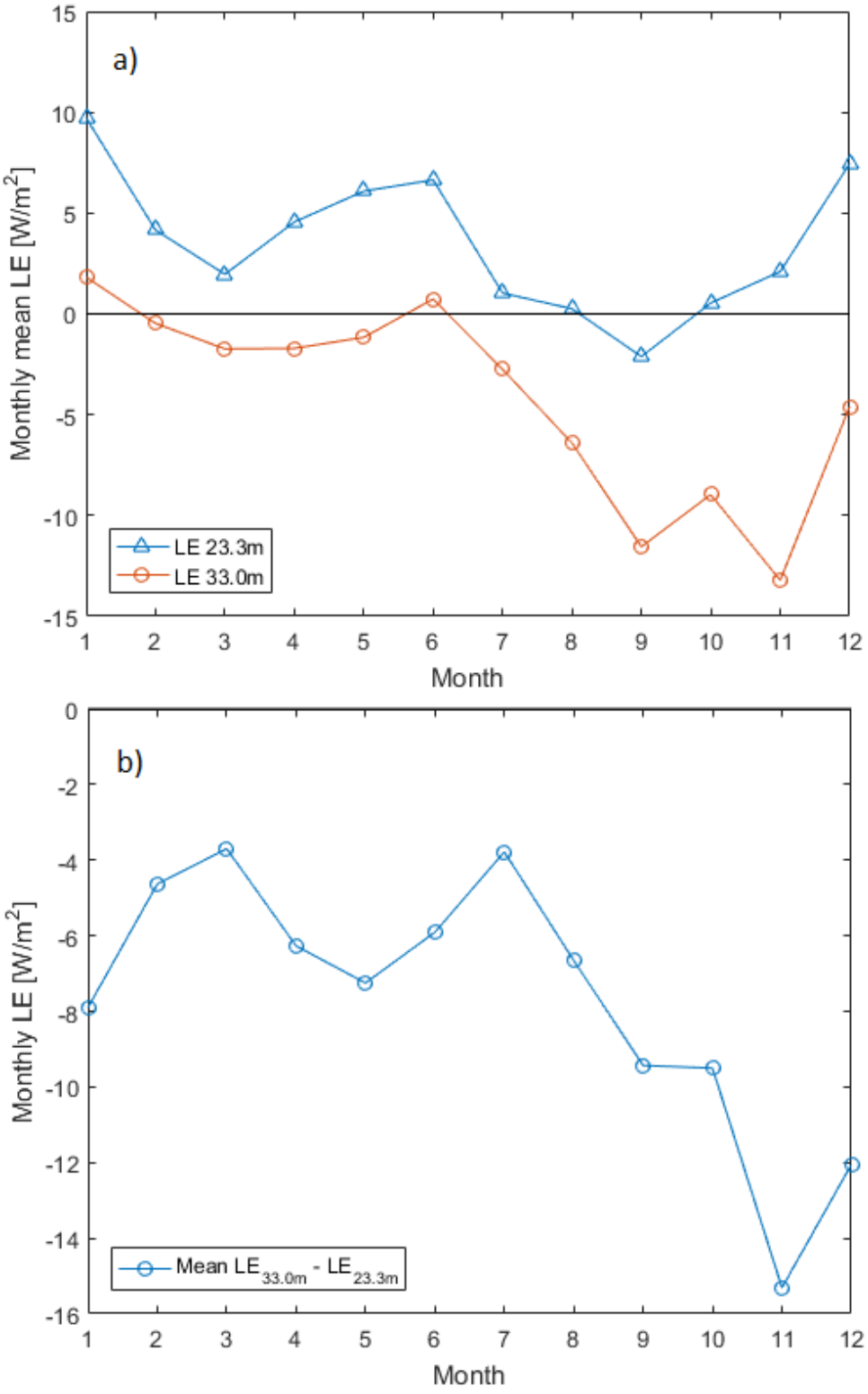

Fig. 4.5 Monthly mean nighttime LE flux in 2015 measured at 23.3 m and 33.0 m (a). Monthly mean nighttime LE difference between the heights (b).

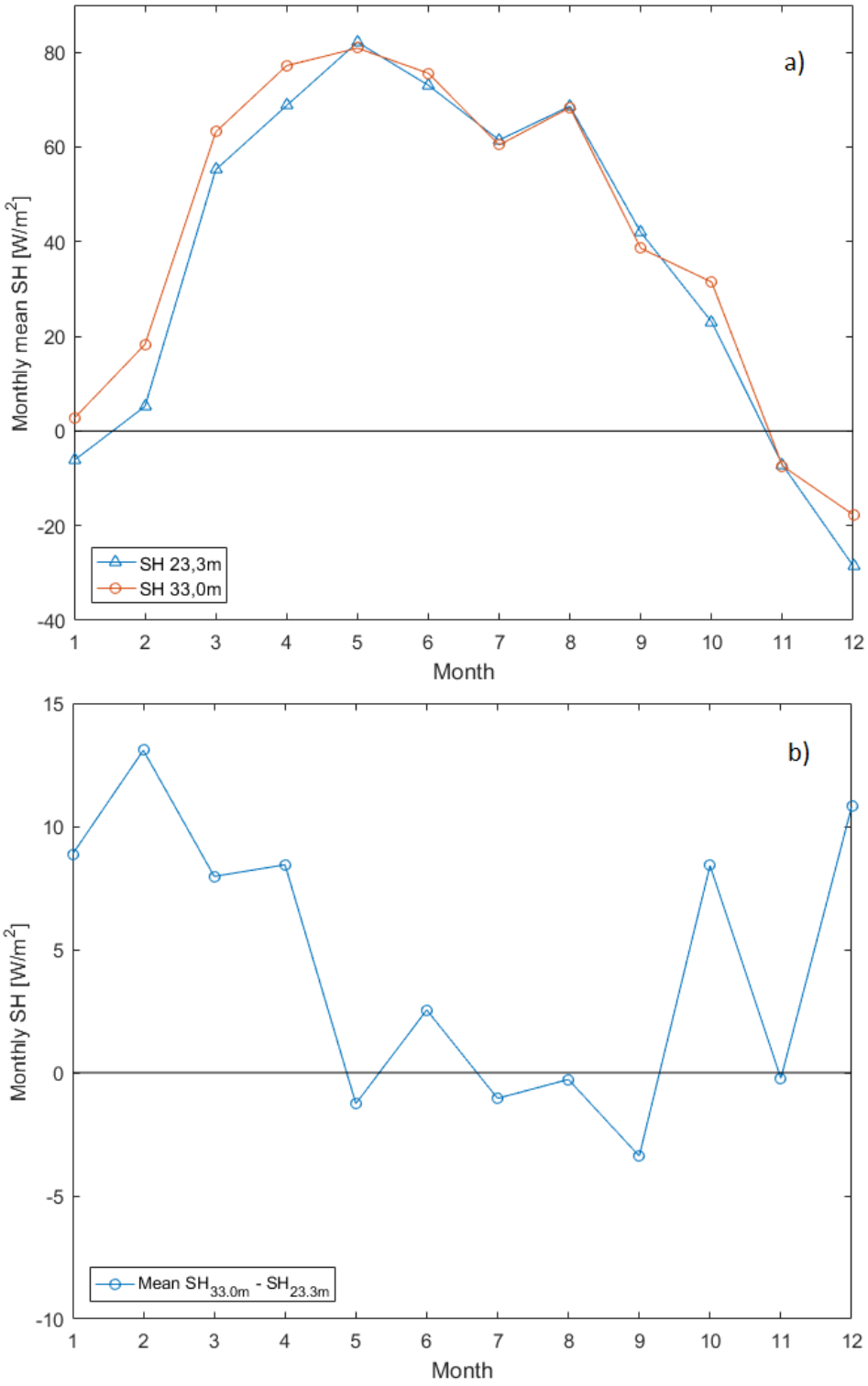

Fig. 4.6 Monthly mean daytime SH fluxes for 23.3 m and 33.0 m (a) and the difference between the monthly values (b).

Monthly mean friction velocity values for 23.3 m and 33.0 m measurement set-ups are similar, both during daytime and nighttime. No real difference related to the seasonal changes can be seen in the figures 4.7 – 4.8. This means that the measurement set-ups are operating in similar meteorological conditions as expected. The friction velocity filtering done with the value $u^* < 0.3\, m\, s^{-1}$ filters out data mostly from July and August nights, but also from other time periods, as the values in Fig. 4.8 are monthly means.

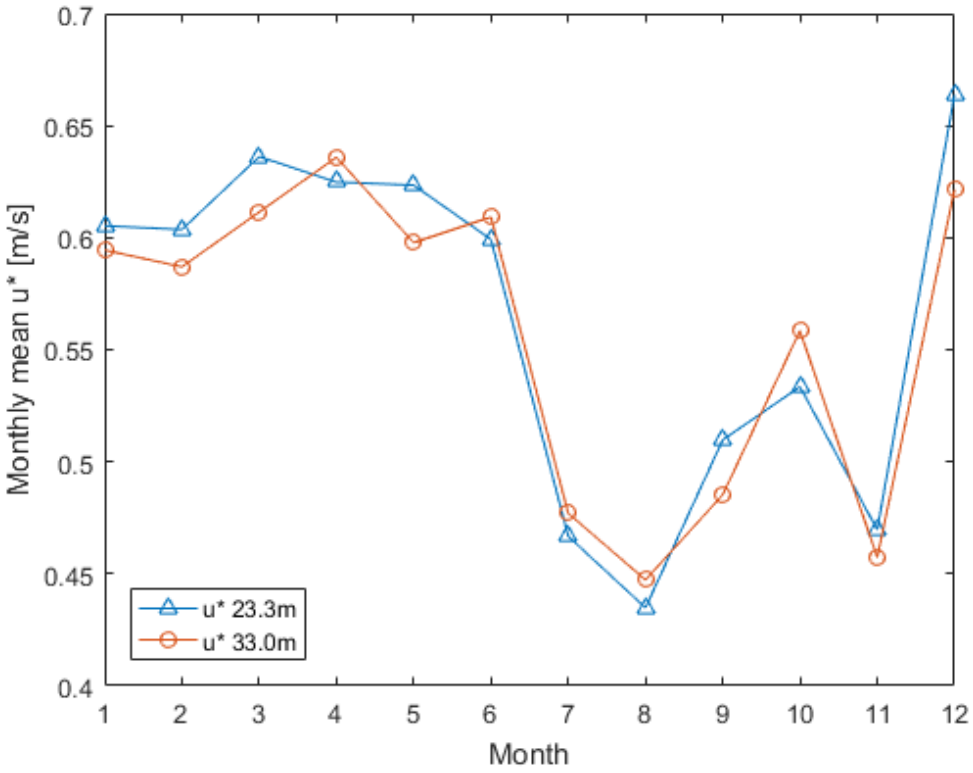

Fig. 4.7 Monthly mean daytime friction velocities in 2015.

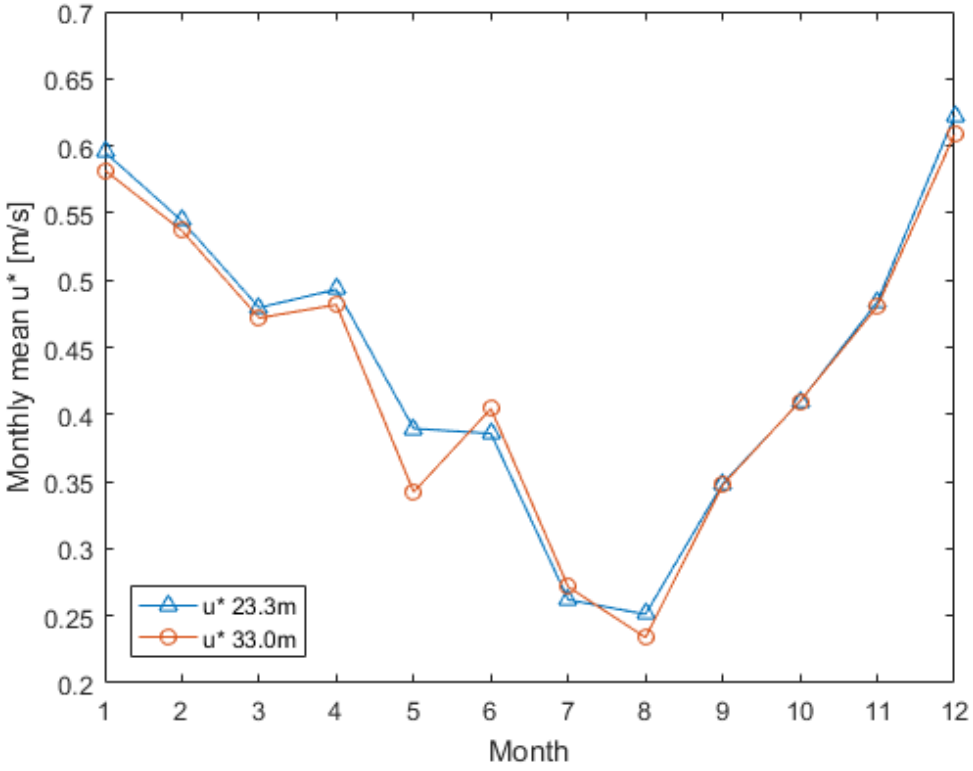

Fig. 4.8 Monthly mean nighttime friction velocities in 2015.

4.2 Diurnal variation

The diurnal variation of NEE, LE and SH flux and friction velocity reveals the usual characteristics of the variables, with both the annual and diurnal cycle of a boreal forest. The diurnal variation is divided into monthly sets in the figures and the hourly values are means of those corresponding to the specific month and time of day.

The diurnal variation of NEE (Fig. 4.9) displays the common characteristics of a boreal forest, with the changes between wintertime and growing season. Negative NEE values represent ecosystem uptake of carbon, and maximum negative values are observed during the midday, as there is a straightforward connection between the amount of insolation and photosynthesis. The maximum uptake is $-15\ \mu mol\ m^{-2}s^{-1}$ during July and the maximum respiration is $7\ \mu mol\ m^{-2}s^{-1}$ also in July, indicating the highest ecosystem activity. In wintertime NEE values remain slightly positive, as photosynthesis no longer occurs in the ecosystem; this is especially true for deciduous forests, but also relevant for evergreens.

The absolute values for NEE, both uptake and respiration, are greater at 33.0 m than at 23.3 m. The difference is about $0.5 - 1\ \mu mol\ m^{-2}s^{-1}$ (10 %) depending on the specific month, which is acceptable for the eddy covariance method. The difference is greatest during the time photosynthesis is occuring (March-September).

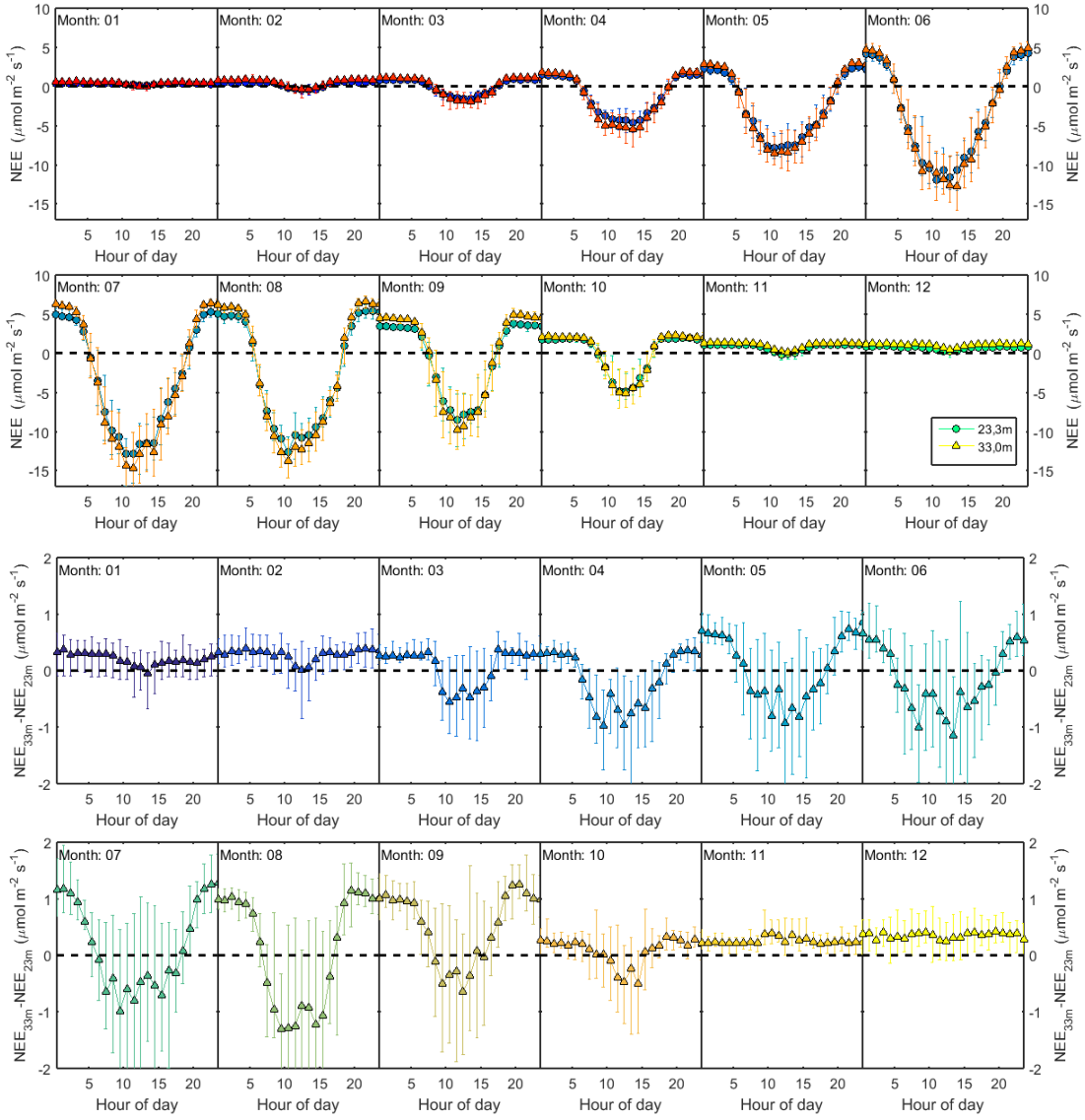

Fig. 4.9 Monthly diurnal NEE exchange measured at 23.3 m and 33.0 m and diurnal difference between the NEE measurements. The error bars present 1 standard deviation for an average period of 1 hour.

The LE values (Fig. 4.10) remain close to zero during winter, which is expected as the temperatures and absolute humidity are low. However the negative values of 33.0 m set-up in November and December are unexpected. The 33.0 m values are lower than the ones from the 23.3 m set-up throughout the year, with the difference

hovering around $-10\ W\ m^{-2}$. The least amount of difference can be seen during March, and the summer months June-August. The difference percentage-wise is largest during winter, with the 23.3 m measurements being almost 100 % bigger than the ones from 33.0 m. The biggest difference in the LE values during May – July can be seen during the morning hours, with almost 20 $W\ m^{-2}$ difference.

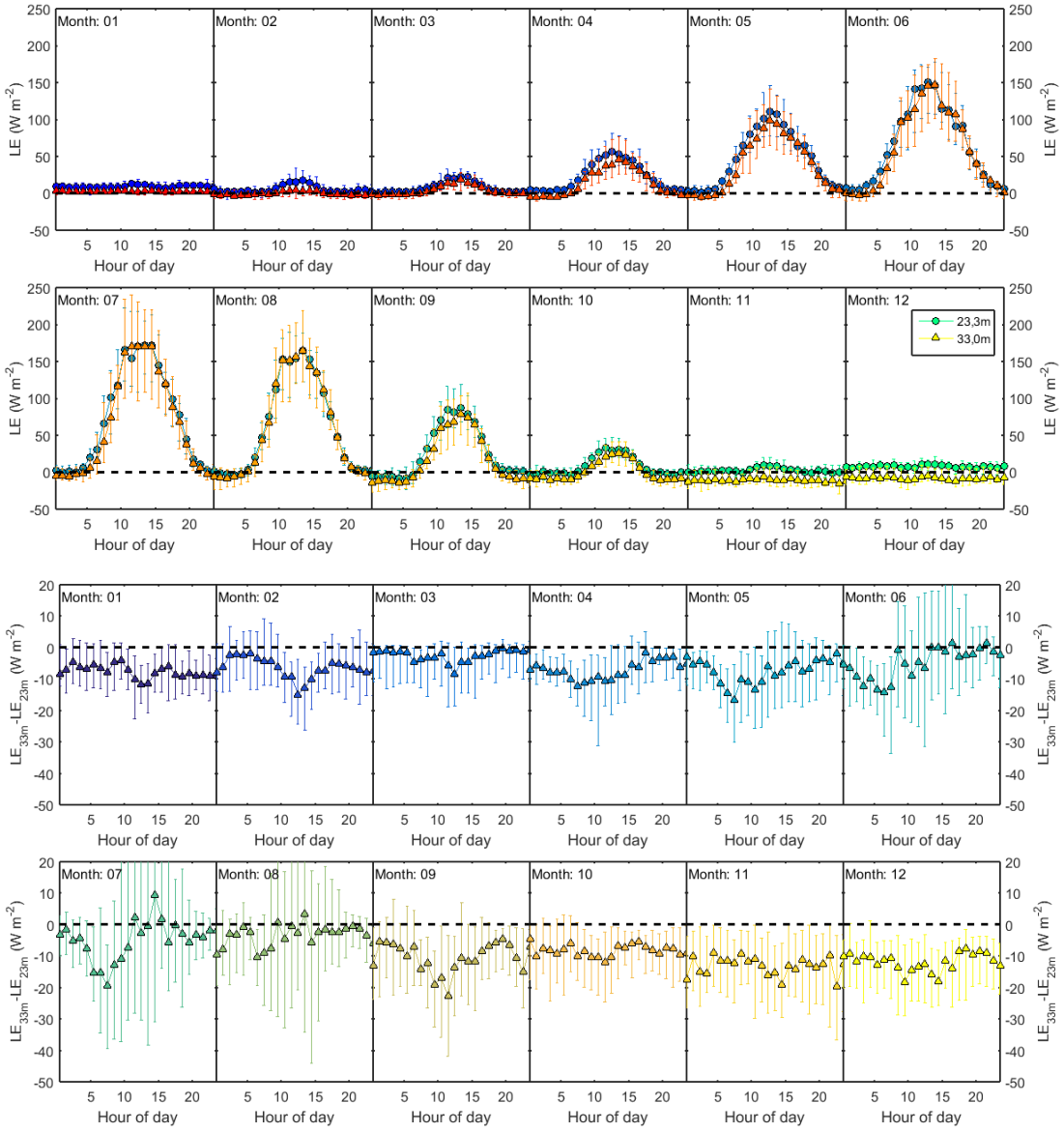

Fig. 4.10 Monthly diurnal LE fluxes measured at 23.3 m and 33.0 m and diurnal difference between the LE measurements. The error bars present 1 standard deviation for 1 hour averaging period.

The diurnal variation of SH fluxes (Fig. 4.11) follow the pattern that is linked to the solar insolation. In February the SH fluxes reach positive values for the first time in midday and the maximum values (200 $W\ m^{-2}$) are observed in June. By the time

winter is coming, the sensible heat fluxes have already been decreasing and, eventually in November, they remain negative during the whole day. The nighttime values remain almost constant through the year ($-20\ W\ m^{-2}$), as they are mainly dependent on the difference between air and surface temperatures, and also on leaf area and snow cover. The difference between the measurement set-ups is negligible, remaining under $20\ W\ m^{-2}$ throughout the year. The difference fluctuates between positive and negative values, which indicates that there are no consistent differences between the measurement set-ups.

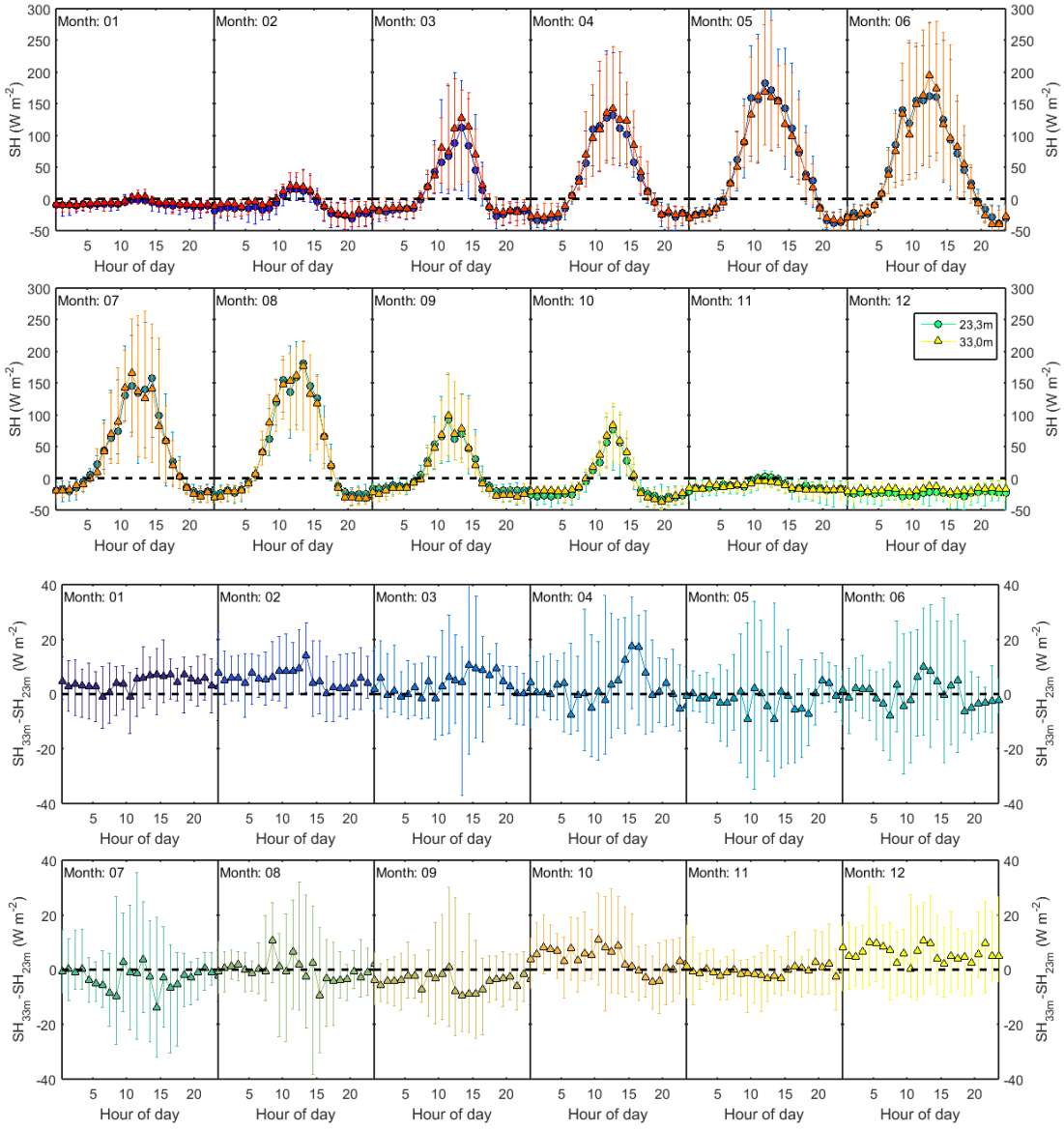

Fig. 4.11 Monthly diurnal SH fluxes measured at 23.3 m and 33.0 m and diurnal difference between the SH measurements. The error bars present 1 standard deviation for 1 hour averaging period.

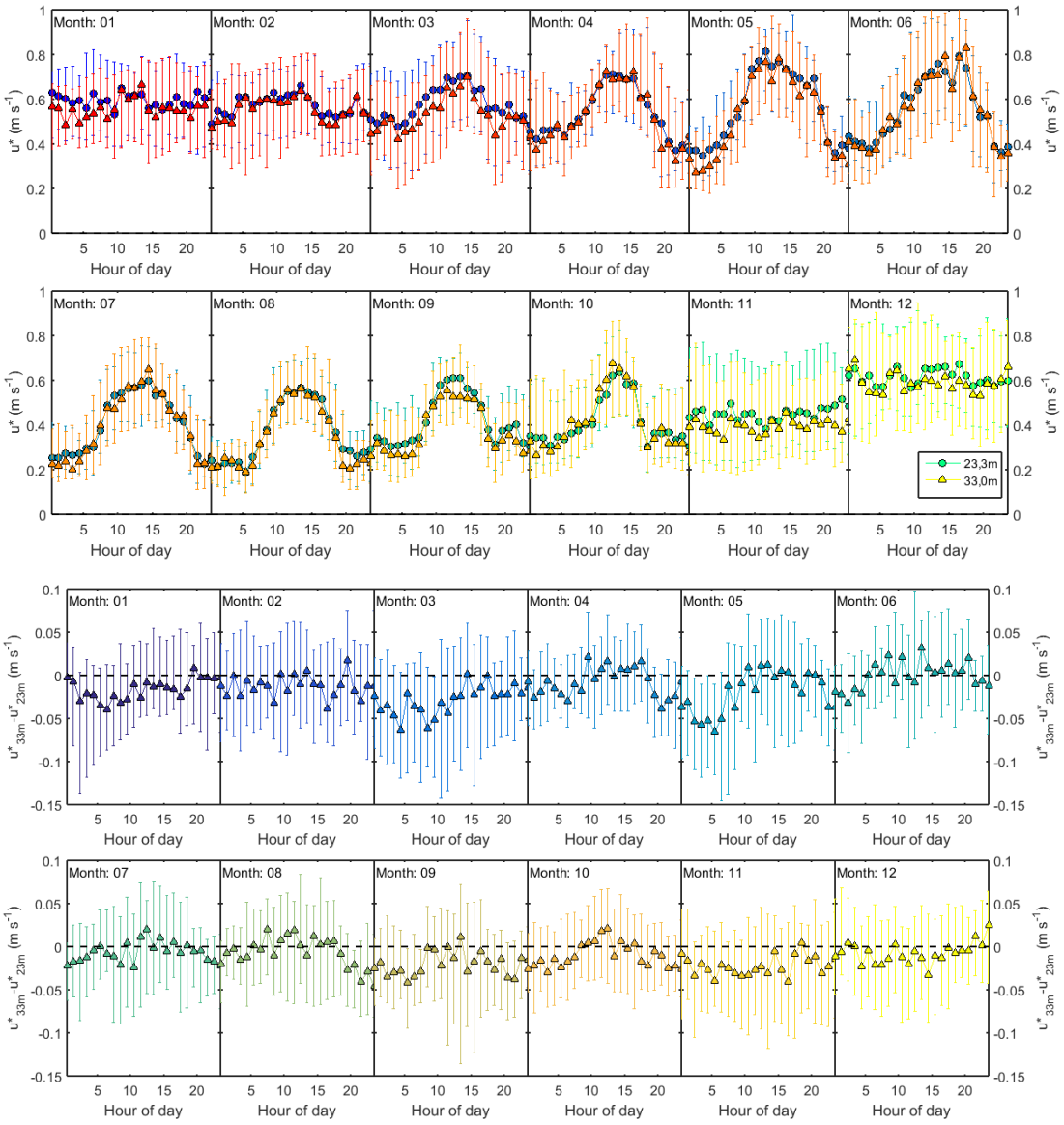

Fig. 4.12 Monthly diurnal friction velocities measured at 23.3 m and 33.0 m and diurnal difference between the u^* measurements. The error bars present 1 standard deviation for 1 hour averaging period.

The diurnal variation of friction velocities (Fig. 4.12) is largest during the summer, as there is more variability in turbulence conditions. The friction velocities do not vary significantly between daytime and nighttime during the winter, but a distinct diurnal variation can be seen in March-October. In the diurnal cycle the friction velocity has a minimum during the night and reaches a maximum in midday. The values measured at 23.3 m are generally speaking slightly greater than those of 33.0 m set-up. However, the difference is quite small, $0.02\ m\ s^{-1}$ /~5 %, proving that both measurement set-ups operate in similar flow conditions.

4.3 Differences due to wind direction

Differences in flux measurements can be caused by the heterogeneities in the underlying surface. The effect of some topographical or vegetation dependent differences can be examined through wind direction based observations. Slight variation of vertical flow between the multiple wind directions is natural due to weather patterns.

Disturbed wind direction caused by the position of the measurement instruments on the side of the measurement tower can be seen between 130° and 220° (Fig. 4.13). However, the distortion does not seem to affect the flux values, as seen with NEE in Fig. 4.14. Similar results with LE and SH fluxes were obtained with no real correlation between them and the wind direction (not shown).

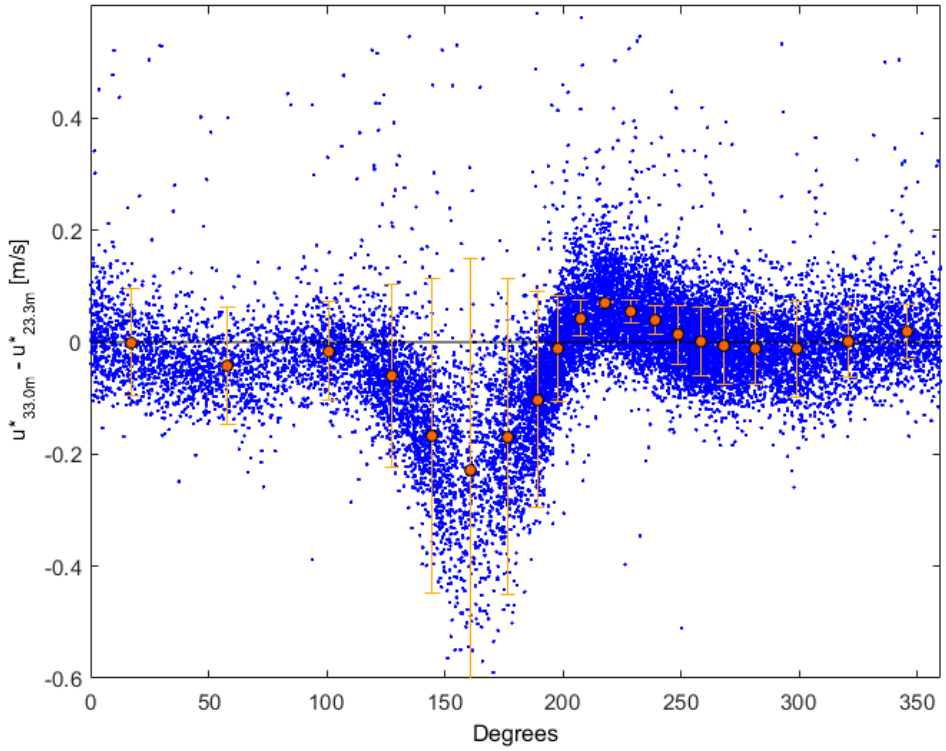

Fig. 4.13 Friction velocity difference in all wind directions over the whole year with bin averages.

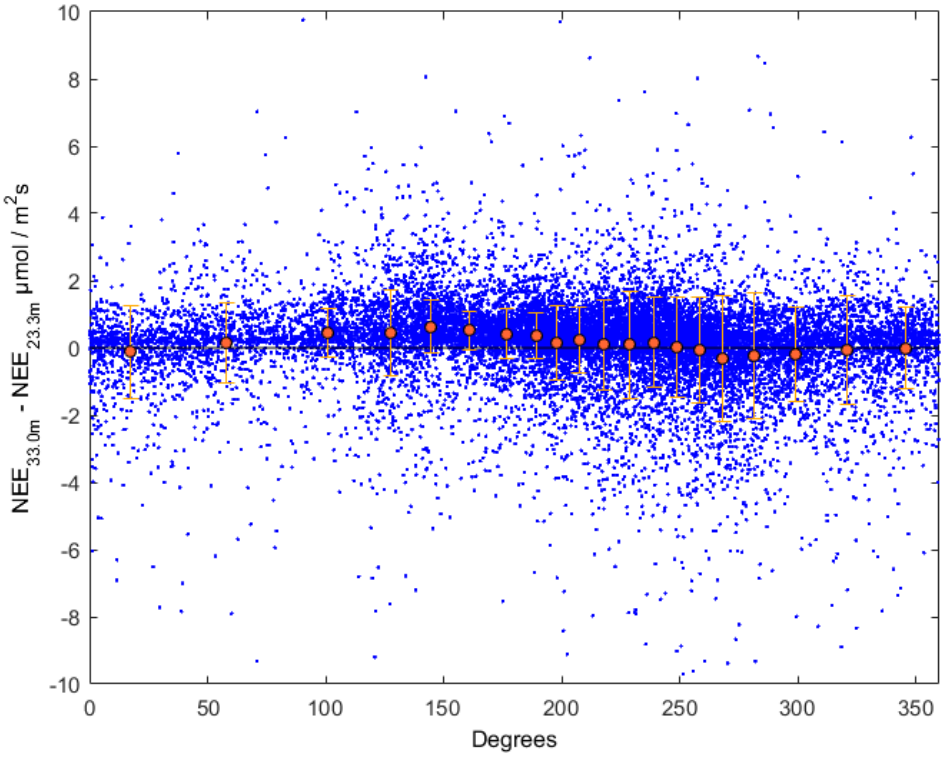

Fig. 4.14 NEE difference in all wind directions over the whole year with bin averages.

4.4 Differences due to atmospheric stability

The stability conditions affect the measurements by implying the amount of mixing occurring in the lower atmosphere. As the measurements are acquired on two different elevation levels above the ground, the effect of turbulence might vary between them. Stability does also affect the footprint characteristics, which is discussed in Sect. 4.5.

The net ecosystem exchange difference between the two measurement set-ups related to the various stability conditions is shown in figure 4.15. For stable conditions NEE values at 33.0 m are larger than those of 23.3 m. For unstable conditions NEE values at 23.3 m are less negative than the measurements acquired at 33.0 m. If we assume that most stable (unstable) conditions happen during nighttime (daytime), we can derive that absolute values of 33.0 m NEE are larger on the majority of stability conditions.

The mean differences seen in figure 4.15 hover around 1 $\mu mol\, m^{-2}s^{-1}$, while the monthly NEE means varies from the winter values of 0.5 $\mu mol\, m^{-2}s^{-1}$ to

midsummer values of $-6\,\mu mol\,m^{-2}s^{-1}$ (Fig. 4.1). The difference is the smallest during the more neutral conditions, although the variation throughout the stability spectrum is quite constant.

The latent heat values for the 23.3 m set-up are larger than those of the 33.0 m set-up during all stability conditions, which can be seen from figure 4.16. The difference between the set-ups is close to zero during the most stable and most unstable conditions, but grows towards the more neutral atmospheric conditions. The maximum averaged difference is about $10\,W\,m^{-2}$ on both instances.

The sensible heat flux difference shown in Fig. 4.17 reveals that both of the measurement set-ups are recording quite similar values during all stability conditions. The SH fluxes are observed to be larger for the 33.0 m set-up during stable conditions and for the 23.3 m set-up during unstable conditions. The difference in both cases is about $10\,W\,m^{-2}$ and the amount of scatter increases towards the more neutral conditions.

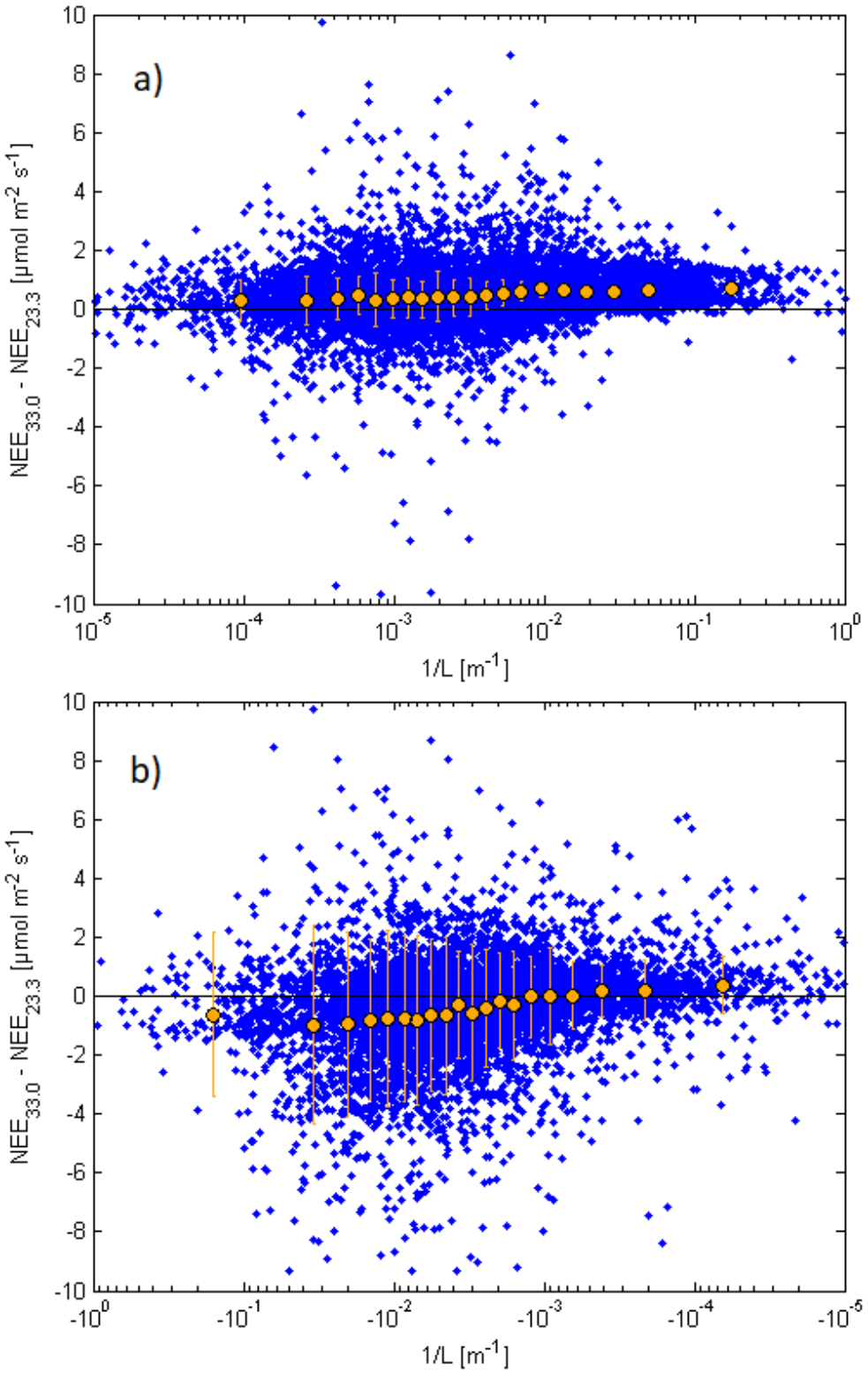

Fig. 4.15 NEE difference in both stable (a) and unstable (b) stability conditions, with bin averages.

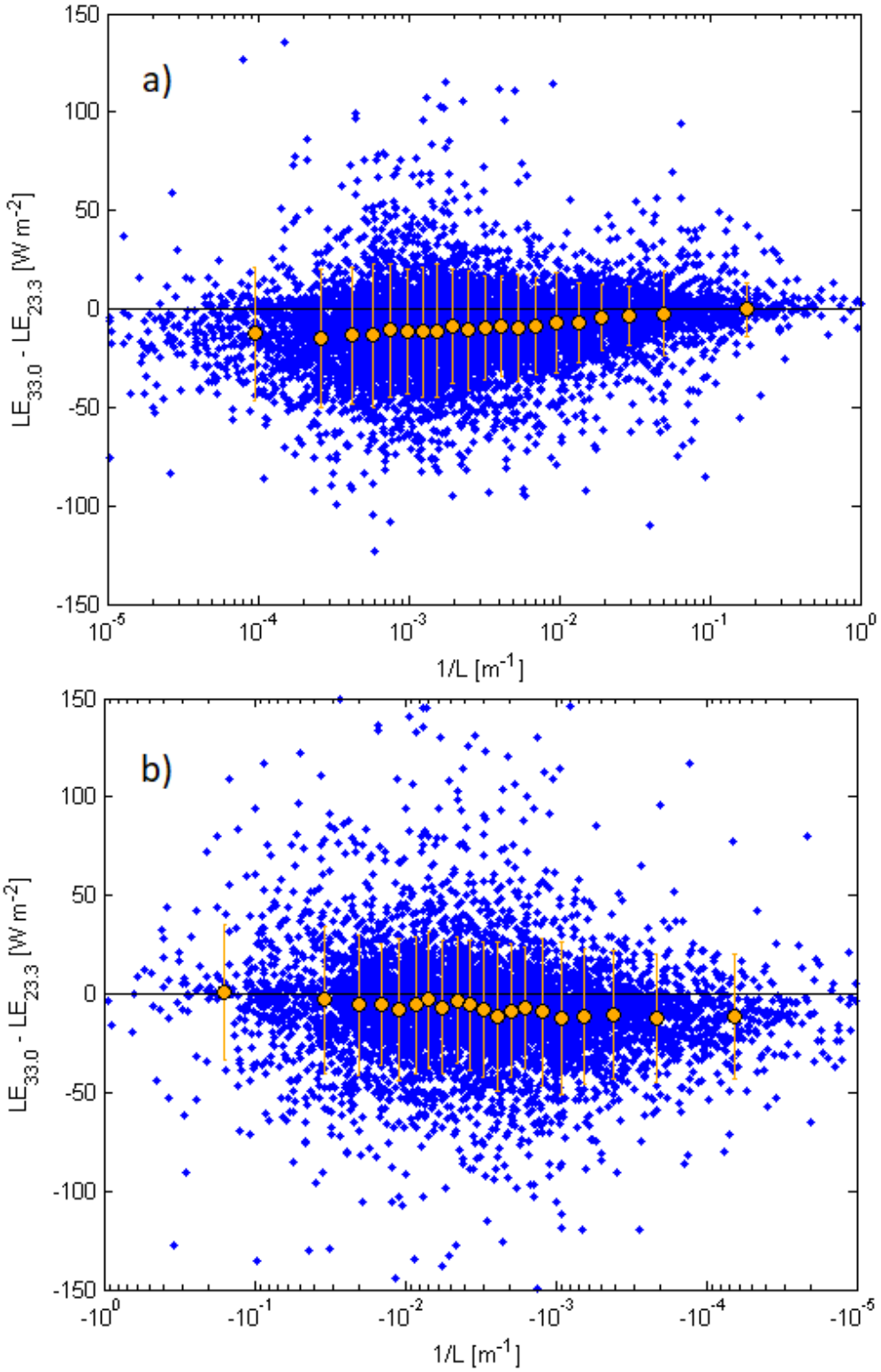

Fig. 4.16 LE difference in all stable (a) and unstable (b) stability conditions, with bin averages.

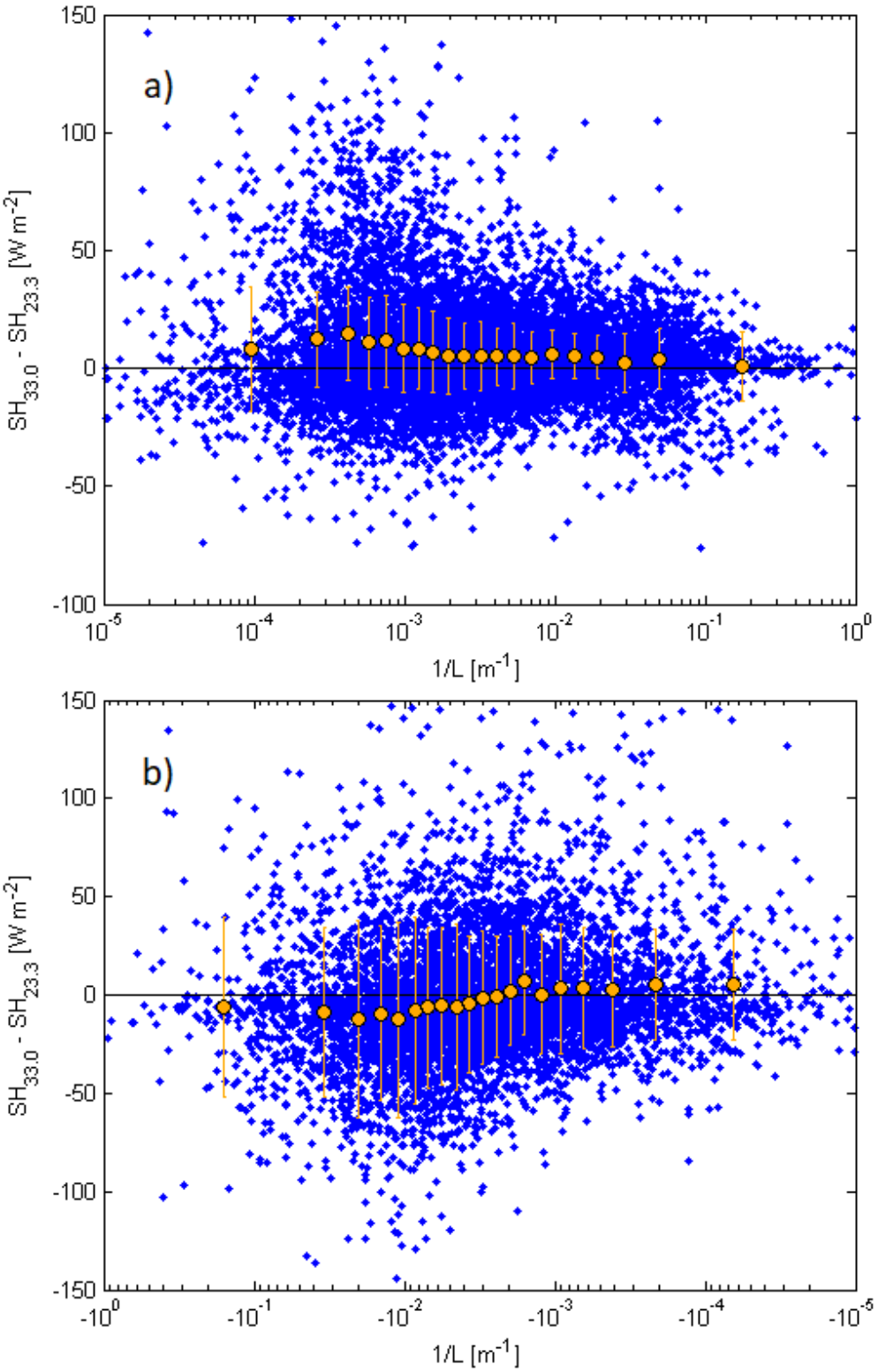

Fig. 4.17 SH difference in stable (a) and unstable (b) stability conditions, with bin averages.

4.5 Footprint analysis

The objective of this analysis is to determine if any differences between the two measurement set-ups is caused by the meteorological or biological phenomena. The footprint analysis tackles both aspects when the vegetation distribution is taken into account. The SMEAR II research station consists mostly of Scots pine (see Sect. 3.1), but a noticeable patch of spruce trees is located south (135° – 210°) of the measurement tower. The closest edge of the spruce patch is located at a distance of 180 m from the measurement tower. The footprint is dependent on the measurement height; the footprint covers larger area when the measurement point is higher. This notion means that the 33.0 m measurement set-up should get more of its flux signal from further away than the 23.3 m measurement set-up, and therefore the amount of difference in flux behavior due to the tree type change at the distance of 180 m can be observed through the footprint analysis.

In the analysis 21 stability scenarios is picked from the stability distribution to represent the common stability conditions observed at the site. The distribution of stability scenarios is shown in Fig. 4.18. Majority of the unstable scenarios fit between values $-10^{-1.5} < 1/L < -10^{-3}$, while most of the stable scenarios lie between $10^{-3.5} < 1/L < 10^{-2}$. The distribution is limited to consider only the south direction at which the spruce patch is located. The data also only includes values that are observed during daytime solar angle of > 10° and nighttime solar angle of < -3° to avoid intermediate conditions. Üllar Rannik implemented a Lagrangian stochastic model on these 10 unstable and 11 stable conditions to simulate the footprint scenarios. The footprint modelling used an approach presented by Rannik et al. (2003) that was applied to ABL and took into consideration the turbulent dispersion within the canopy. The footprint scenarios are analyzed at the 90 % cumulative contribution level and at the distance of 180 m.

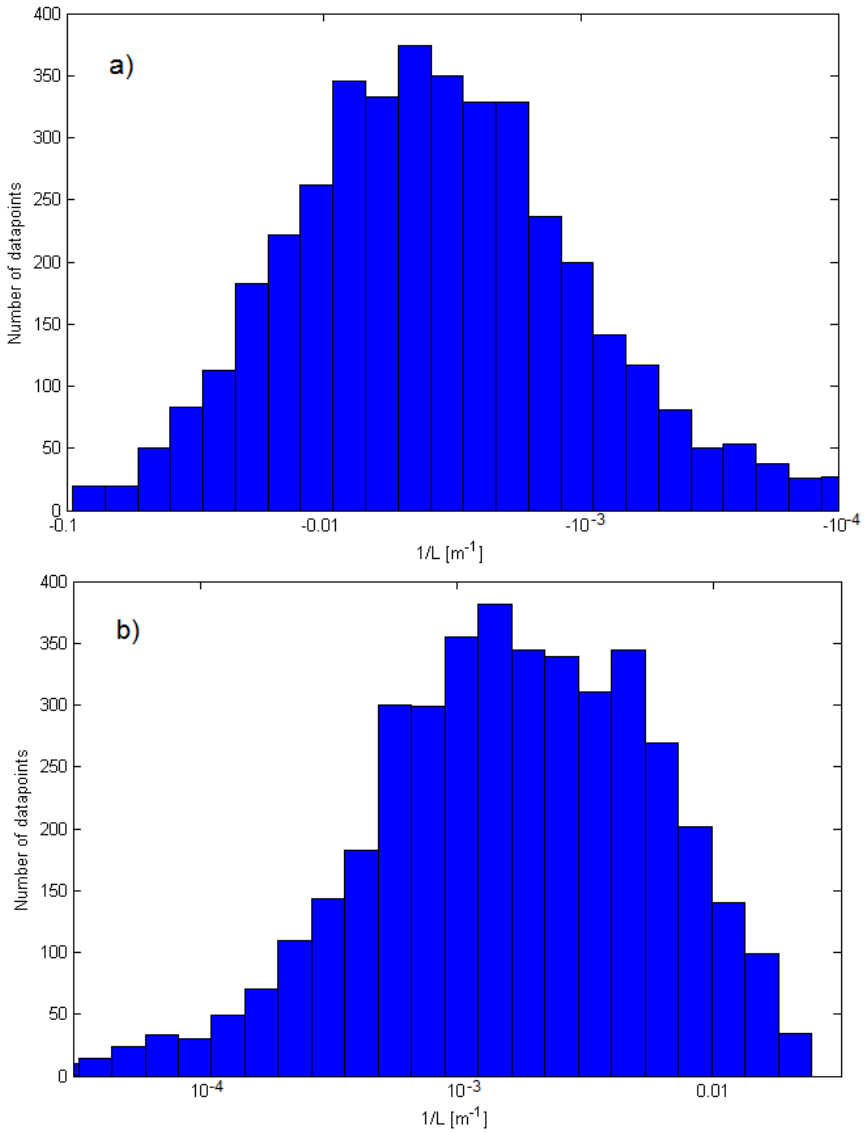

Fig. 4.18 The amount of unstable (a) and stable (b) half hour runs recorded at 23.3 m, the 33.0 m set-up has a similar distribution.

In Fig. 4.19 the footprint difference is clearly visible between the two measurement heights. The unstable values form a tighter spread with higher cumulative footprint values, while the stable cumulative footprint values grow slower with the distance. This behavior is fully expected, as discussed in Sect. 2.4. The distance from the measurement tower is normalized with the tree height 18 m in the Fig. 4.19. The 21 different stability scenarios are representing the distribution of meteorological conditions observed at the measurement site. The unstable scenarios were modelled with the source height being $\frac{3}{4}$ of the canopy height, while the stable scenarios had source height set on the ground level.

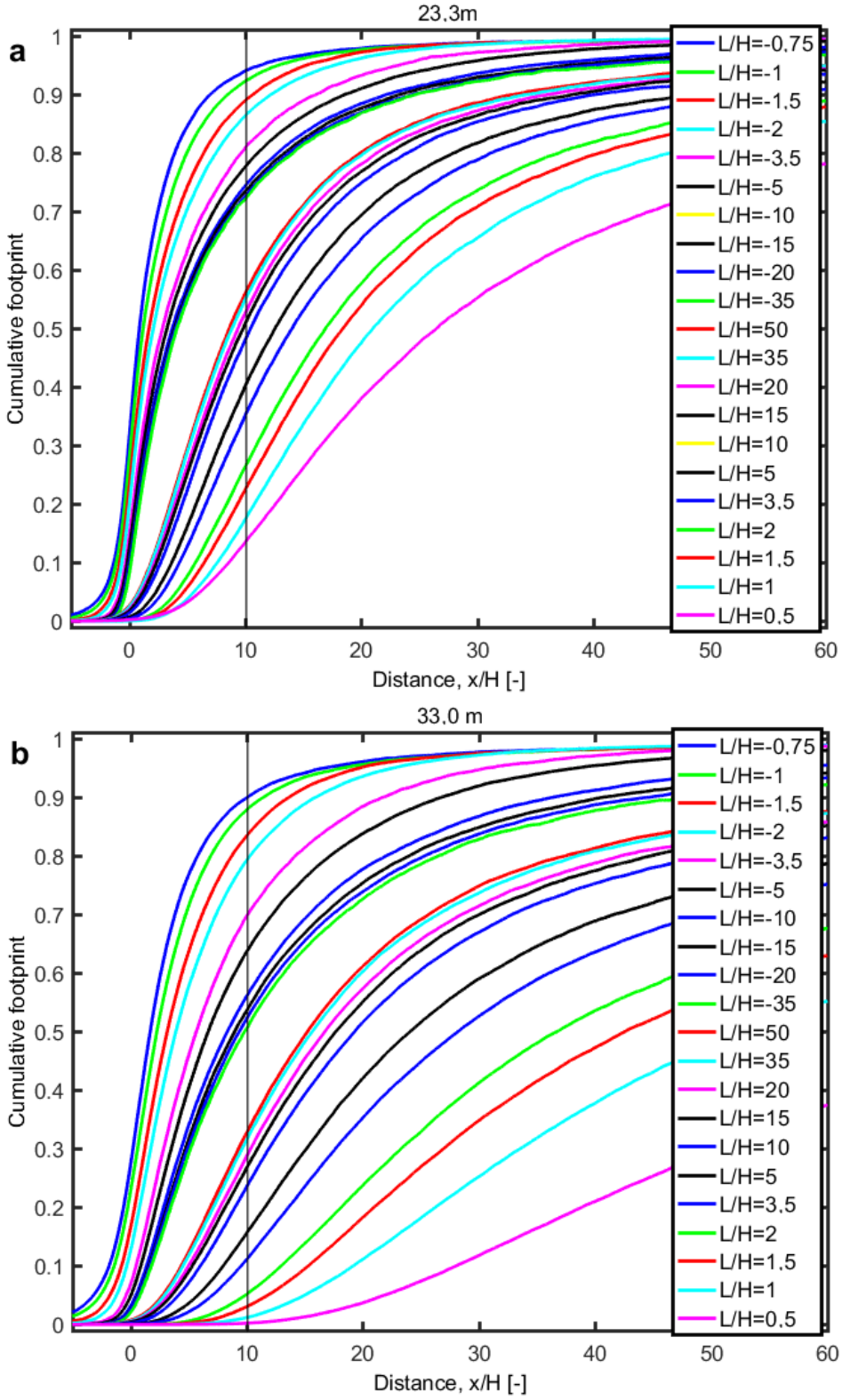

Fig. 4.19 Cumulative flux footprints for 23.3 m (a) and 33.0 m (b). The distance from the measurement tower and the stability parameter (Obukhov length L) are normalized with the canopy height ($H = 18m$). Negative L/H values correspond to unstable scenarios and positive L/H values to stable scenarios. The distance at which the pine forest changes into spruce forest in the south is indicated in the figures ($x/H = \frac{180m}{18m} = 10$).

In table 4.2 the Fig. 4.19 is further analyzed, with the notion that friction velocity filtering (Sect. 3.3.1) is done with $u^* < 0.3\ m\ s^{-1}$, thus excluding some of the most stable scenarios. The contribution difference varies from 0.3 p.p. to 27.2 p.p. for the most unstable and fairly stable scenarios, respectively. For slightly stable conditions the difference of contribution to 90 % cumulative footprint between the two measurement heights is around 25 p.p. At 90 % cumulative footprint level, during unstable and neutral conditions, the 23.3 m set-up acquires 80 % or more of its flux from the pine forest in the south direction, while the 33.0 m set-up acquires only 56 % or more of its flux from the studied pine forest sector.

Obukhov length 1/L [1/m]	Cumulative footprint percentage at 180 m distance [%] **23.3 m**	Contribution of pine forest to 90 % cumulative footprint [%] **23.3 m**	Cumulative footprint percentage at 180 m distance [%] **33.0 m**	Contribution of pine forest to 90 % cumulative footprint [%] **33.0 m**	Contribution difference **23.3 m - 33.0 m** [p.p.]
Unstable					
$-10^{-1,15}$	93.9	100.0	89.75	99.7	0.3
$-10^{-1,25}$	92.2	100.0	87.75	97.5	2.5
$-10^{-1,45}$	88.8	98.7	83.25	92.5	6.2
$-10^{-1,55}$	86.25	95.8	79	87.8	8.1
$-10^{-1,80}$	80.75	89.7	69.75	77.5	12.2
$-10^{-1,95}$	77.5	86.1	63.5	70.6	15.6
$-10^{-2,25}$	74.3	82.6	56	62.2	20.3
$-10^{-2,40}$	73.4	81.6	53.5	59.4	22.1
$-10^{-2,55}$	72.5	80.6	52	57.8	22.8
$-10^{-2,80}$	72	80.0	50.5	56.1	23.9
Stable					
$10^{-2,95}$	56	62.2	32.5	36.1	26.1
$10^{-2,80}$	55	61.1	31.5	35.0	26.1
$10^{-2,55}$	52.5	58.3	28.75	31.9	26.4
$10^{-2,45}$	51	56.7	26.75	29.7	26.9
$10^{-2,25}$	48	53.3	23.5	26.1	27.2
$10^{-1,95}$	40	44.4	15.5	17.2	27.2
$10^{-1,80}$	35	38.9	11	12.2	26.7
$10^{-1,55}$	26.5	29.4	5	5.6	23.9
$10^{-1,45}$	22.5	25.0	3	3.3	21.7
$10^{-1,25}$	17.25	19.2	1	1.1	18.1
$10^{-0,95}$	13.5	15.0	0.2	0.2	14.8

Table 4.2 The effect of stability variation to the contribution of pine forest to 90 % cumulative footprint in south, where the vegetation changes into spruce forest at a distance of 180 m from the measurement tower. Four of the most stable scenarios are filtered out of the data in post-processing.

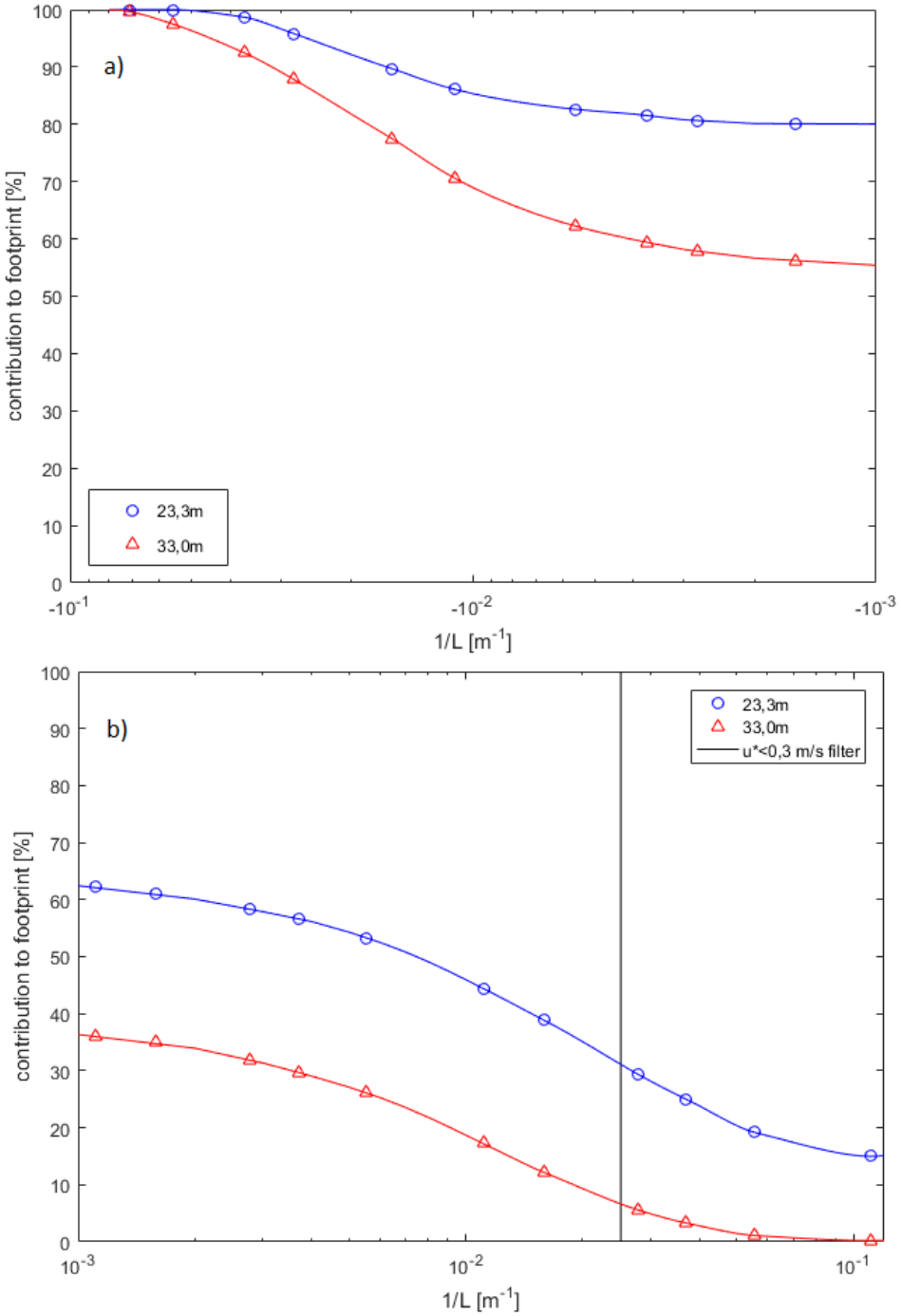

Fig. 4.20 Estimation of the contribution of pine forest to the 90% footprint for unstable (a) and stable (b) scenarios. Scenarios that are beyond (more stable) the u^* filtering, are not used in the flux analysis (see Sect. 3.3.1).

Fig. 4.20 visualizes the contribution of pine forest to 90 % footprint during most of the atmospheric stability conditions observed at the SMEAR II site. The difference between the two measurement heights seems to be largest during slightly stable

conditions ($|1/L| < 10^{-3}\ m^{-1}$), and the smallest during most unstable conditions. The measurement set-ups at 23.3 m and 33.0 m at SMEAR II site are designed to represent the Scots pine forest, and from Fig. 4.20 the level of representativeness during various stability conditions can be distinguished. Note that the Scots pine forest extends further away (a few kilometers) in most of the directions, and that the footprint analysis considers only the change to spruce forest in the south direction.

4.6 Cumulative ecosystem exchange

The cumulative ecosystem exchange reveal the characteristics of the underlying ecosystem by for example showing how big of a carbon source or sink it annually is. It is also a useful way of determining how large the difference between multiple measurement set-ups is annually.

The cumulative net ecosystem exchange of 23.3 m and 33.0 m set-ups have similar behavior through the year 2015 (Fig. 4.21). Both of them depict the cumulative ecosystem respiration during January-March and October-December, when there is not enough insolation to allow photosynthesis in the boreal vegetation. However a difference in the amount of respiration can be observed from the figure 4.21 and based on figure 4.22 it is evident that the 33.0 m measurement set-up is gathering higher respiration values than the 23.3 m set-up. During the growing season no real difference in the cumulative NEE values can be observed. The annual cumulative NEE in units grams of carbon per square meter at the 23.3 m set-up is $-294\ gC\ m^{-2}$ and at the 33.0 m set-up $-245\ gC\ m^{-2}$, proving that the Scots pine forest acts as a carbon sink. The cumulative difference between the measurement set-ups is $49\ gC\ m^{-2}$, which is at a satisfying accuracy level ~ 20 % (Baldocchi, 2003). The result demonstrates that the two measurement set-ups are portraying the same ecosystem with similar micrometeorological characteristics.

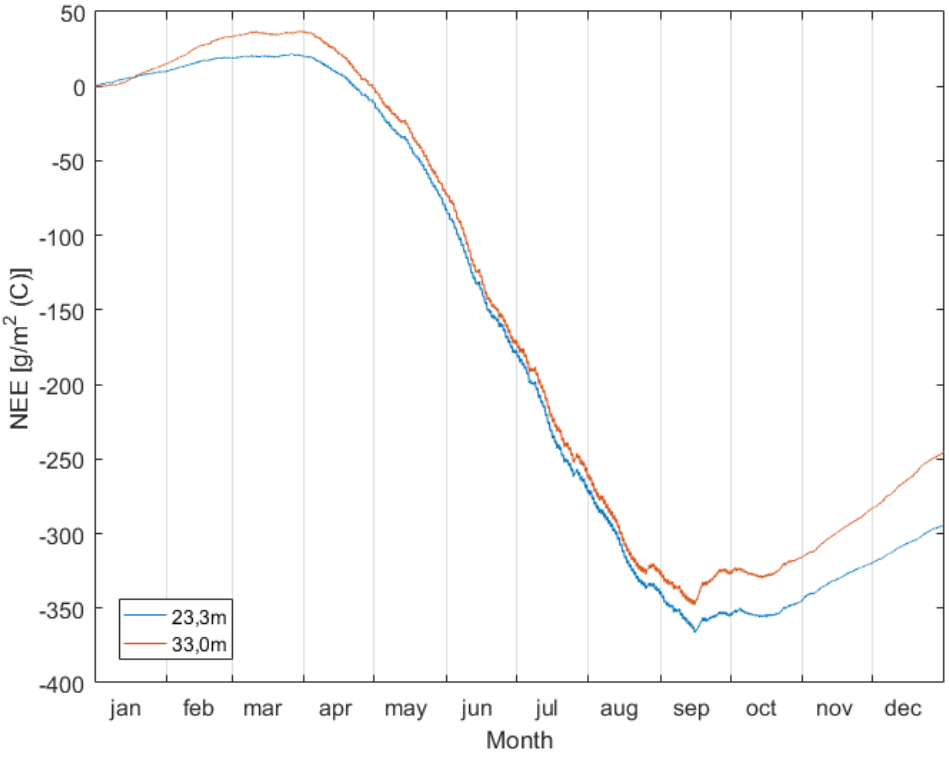

Fig. 4.21 Cumulative NEE on the 23.3 m and the 33.0 m set-ups over the year 2015.

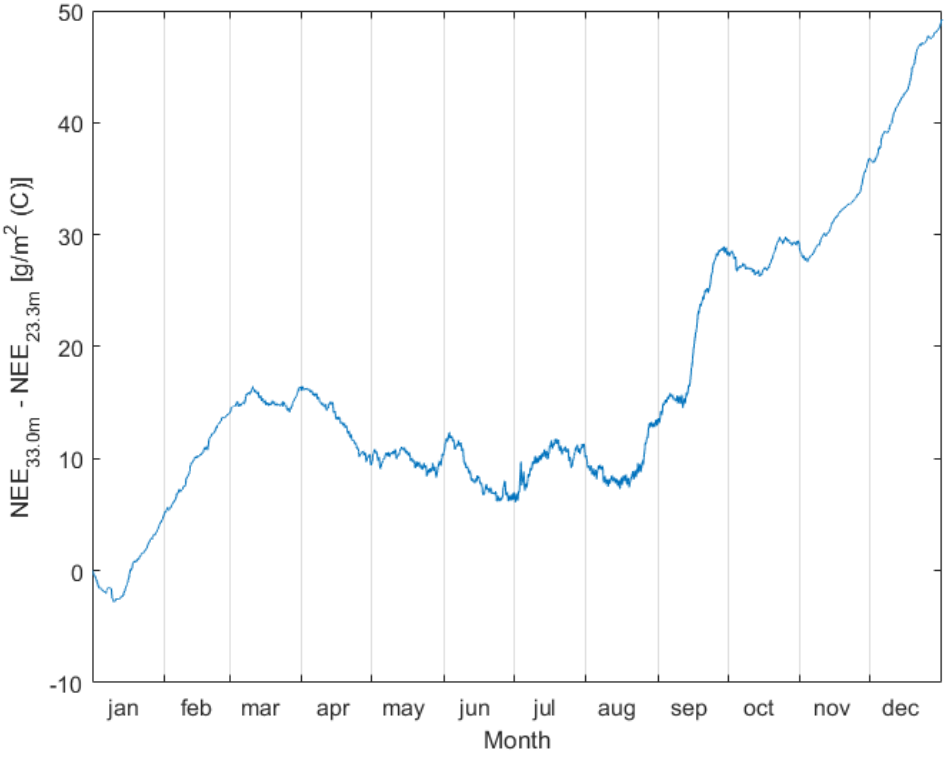

Fig. 4.22 Cumulative NEE difference over the year 2015.

The ecosystem respiration and uptake were both larger in the 33.0 m measurements (Fig. 4.2 – 4.3), but they cancel out each other's effect on NEE during summer, leaving a small difference between the set-ups. However, in the wintertime, when there is only ecosystem respiration, the larger values of 33.0 m compared to the ones from 23.3 m show up in the cumulative NEE.

The annual cumulative LE values are shown in Fig. 4.23 for the 23.3 m measurement set up and 33.0 m measurement set-up. The results show that the 33.0 m set-up is collecting lower LE values continuously throughout the year. The annual cumulative LE for the 23.3 m set-up is 362 mm and for the 33.0 m set-up 257 mm, while the difference being 105 mm, meaning that the cumulative value at the 33.0 m is 29 % smaller.

From figure 4.24 it can be seen that the cumulative difference between the measurement set-ups grows almost constantly through the whole year, with hardly any moments where the 33.0 m values are larger than those of 23.3 m.

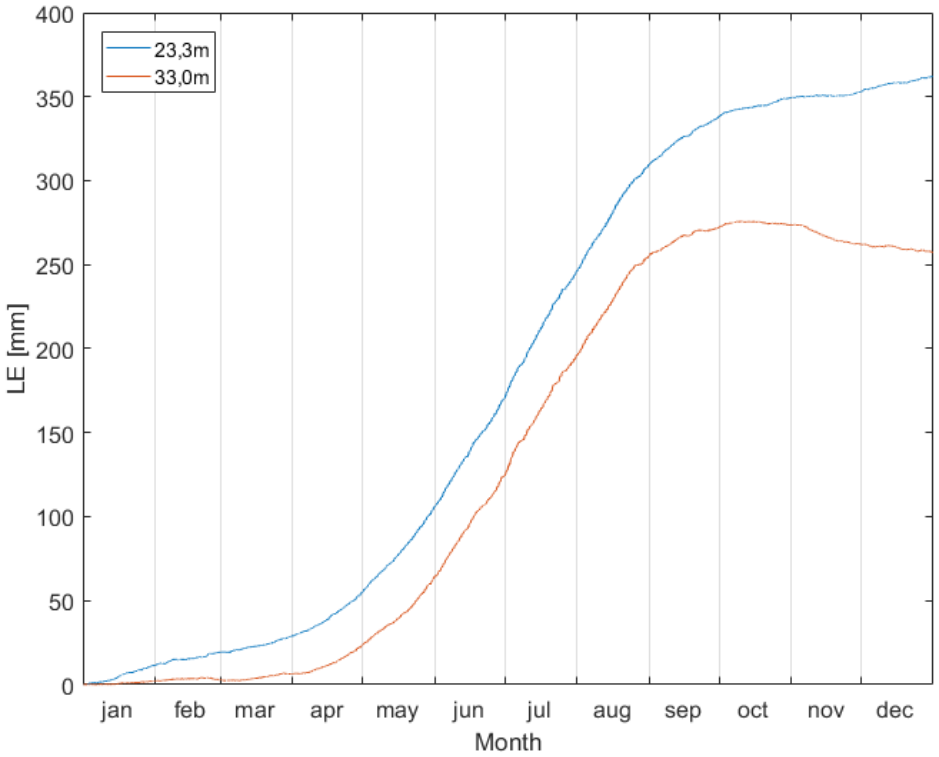

Fig. 4.23 Cumulative LE on the 23.3 m and the 33.0 m set-ups during the year 2015.

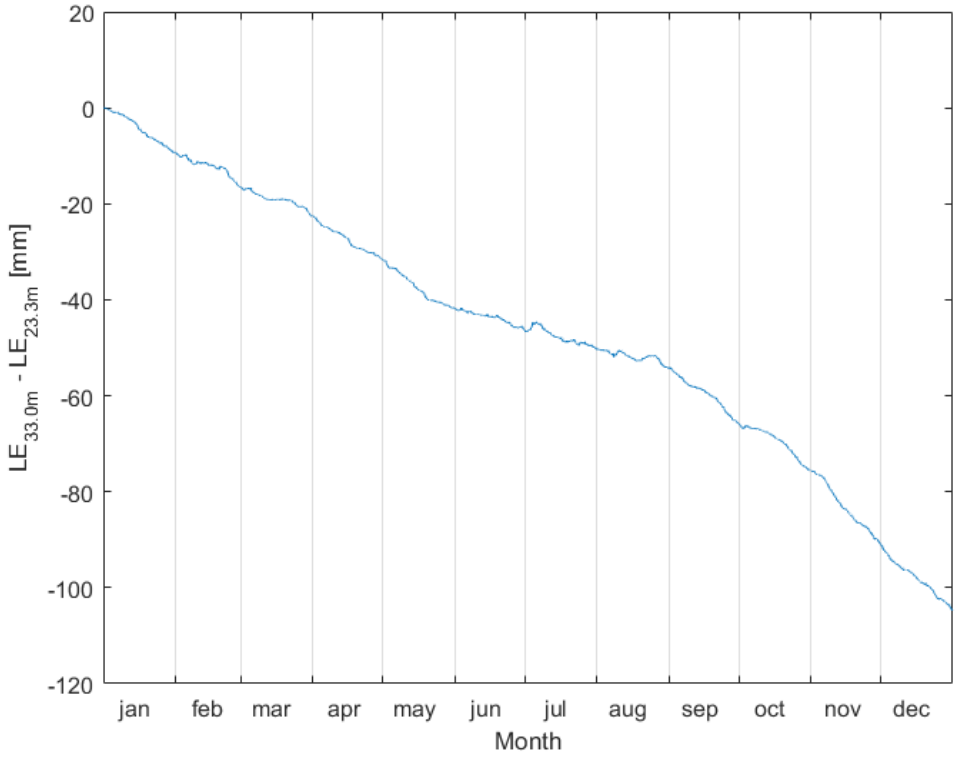

Fig. 4.24 Cumulative LE difference during the year 2015.

5. CONCLUSIONS

The aim of this study was to determine the level of uncertainty in forest–atmosphere exchange while using eddy covariance measurement technique, and to further determine if the observed deviations could be linked with micrometeorological or flux footprint related variations or if they were resulted by the uncertainties linked to the measurement system.

The two measurement set-ups seem to operate in similar micrometeorological setting, as the differences in friction velocities and wind patterns are small. The proximity of the canopy top does not have an effect on the lower measurement set-up, even though it is located only ~ 5 m above the canopy. There are no noticeable differences in sensible heat measurements between the two heights and they both showcase the 1.5 – 2.0 °C colder average temperatures of June and July (Finnish Meteorological Institute).

The ecosystem is observed to be a carbon sink as expected, because the pine trees are still growing. The annual cumulative net ecosystem exchange (NEE) are estimated to

be $-294\ gC\ m^{-2}year^{-1}$ at the 23.3 m measurement height and $-245\ gC\ m^{-2}year^{-1}$ at the 33.0 m measurement height, respectively. A long-term ecosystem carbon balance study (Ilvesniemi et al., 2009) conducted at the same SMEAR II location (23.3 m set-up), showed an average annual NEE of $-206\ gC\ m^{-2}year^{-1}$ during 1995-2008.

The annual cumulative difference of NEE between the two measurement heights is estimated to be 49 $gC\ m^{-2}year^{-1}$ (~ 17 % difference), which is in the same ballpark with the total uncertainty of long term EC measurements ($\pm 50\ gC\ m^{-2}year^{-1}$) for measurements at nearly ideal sites (Baldocchi, 2003). A recent study (Rannik et al., 2006) was conducted in the same measurement station, and showed an estimation of annual cumulative NEE difference of 80 $gC\ m^{-2}year^{-1}$ between two EC systems located at the same height (23 m) but with a horizontal separation of 30 m.

The difference in NEE between the two measurement heights can be seen for example in the monthly diurnal values, where larger ecosystem respiration values are measured at the 33.0 m set-up during the winter months (November – February). A model is used to determine the total ecosystem respiration (TER), which has a greater effect on the NEE percentage-wise more during the winter time.

However, the LE fluxes measured at the two set-ups do not have as strong correlation with each other as the CO_2 fluxes do. The values of 33.0 m set-up are smaller throughout the year in all atmospheric conditions, while comparing to the 23.3 m values. This creates a constant difference to the flux comparison between the measurement set-ups.

The annual cumulative values of evapotranspiration are 362 mm for the 23.3 m set-up and 257 mm for the 33.0 m set-up. The annual cumulative evapotranspiration difference of 105 mm (29 % difference) is much bigger than what is seen with NEE. The LE measured at 33.0 m behaved peculiarly during November and December with negative values as if there had been condensation of water vapor at the site. Even if the cumulative difference might be considered acceptable, the problem is that the difference does not seem to arise from any specific micrometeorological phenomena, but could be a measurement system related complication.

The negative LE values that were observed at the 33.0 m measurement set-up may suggest that condensation of water is occurring at the measurement site. This is

unusual especially during winter when the temperatures are below freezing and the absolute humidity is low. The negative LE values are usually caused by the lack of sample line heating, enabling condensation inside the sampling tube. When the unexpected negative LE values were seen while analyzing the measurement data in autumn of 2016, the heating of the 33.0 m set-up sample line was checked. The sample line had proper heating then, but from that information no real closure can be made about the sample line being heated throughout the year 2015.

Another origin for the lower than usual LE values can be dirty interior walls of the sampling tube, which is affecting the flow through the tube. This dirtiness leads to a greater attenuation of high frequency fluctuations in water vapor concentrations, which can be seen in the underestimation of LE (Gholz 2002). However, the sampling tubes are cleaned regularly and the sampling tube length is only 0.77 m on the 33.0 m measurement set-up, while it is 7 m on the 23.3 m set-up. The possible flux attenuation caused by dirty sampling tube would be much greater in the longer tube, but the results suggest the opposite.

The footprint analysis shows that in south direction (130° – 200°), where the vegetation changes from pine to spruce, during all atmospheric conditions the 23.3 m set-ups source area is more often inside the pine forest than with the 33.0 m set-up. At 90 % cumulative footprint level, during unstable and neutral conditions, the 23.3 m set-up acquires just 80 % of its flux from the pine forest in the south direction, while the 33.0 m set-up acquires just 56 % of its flux from the same pine forest sector. However, this difference in vegetation does not seem to affect the annual carbon budget or the heat fluxes. Neither were there any real correlation found between wind direction and the CO_2 or energy fluxes.

The measurement height does not seem to influence significantly the flux estimations made with the eddy covariance method, when the measurement set-ups are located at the heights of 23.3 m and 33.0 m over the SMEAR II field measurement station. Exception being the LE flux, but it is not clear how large part of the seen differences in the results is caused by the measurement height or the measurement system.

REFERENCES

Aubinet M et al., 2000. Estimates of the annual net carbon and water exchange of European forests: the EUROFLUX methodology. Adv. Ecol. Res. 30:113-175.

Aubinet M, Vesala T, Papale D, Eds., 2012. Eddy covariance, a practical guide to measurement and data analysis. Springer Atmospheric Sciences.

Baldocchi D 2003. Assessing the eddy covariance technique for evaluating carbon dioxide exchange rates of ecosystems: past, present and future. Glob. Chang. Biol. 9:479-492.

Foken T, 2006. 50 years of the Monin-Obukhov similarity theory. Boundary-Layer Meteorology 119:431–447.

Foken T, 2008. Micrometeorology. Berlin: Springer.

Gholz H, Clark K, 2002. Energy exchange across a chronosequence of slash pine forest in Florida. Agr. Forest Meteorol. 112:87-102.

Goulden M et al. 1996. Measurements of carbon sequestration by long-term eddy covariance: methods and a critical evaluation of accuracy. Glob. Change. Biol. 2:169-182.

Ilvesniemi H et al., 2009. Long-term measurements of the carbon balance of a boreal Scots pine dominated forest ecosystem. Boreal Environment Research 14:731–753.

Kaimal J, Finnigan J, 1994. Atmospheric boundary layer flows: their structure and measurement. Oxford: Oxford University Press.

Kolari P et al. 2009. CO_2 exchange and component CO_2 fluxes of a boreal Scots pine forest. Boreal Environment Research 14:761-783.

Lee X 1998. On micrometeorological observations of surface-air exchange over tall vegetation. Agr. Forest Meteorol. 91:39-49.

Lofgren B, Zhu Y, 2000. Surface energy fluxes on the Great Lakes based on satellite-observed surface temperatures 1992 to 1995. J. Great Lakes Res. 26(3):305-314.

Mammarella I et al., 2009. Relative humidity effect on the high frequency attenuation of water vapour flux measured by a closed path eddy covariance system. Journal of Atmospheric and Oceanic Technology 26:1856-1866.

Mammarella I et al. 2016. Quantifying the uncertainty of eddy covariance fluxes due to the use of different software packages and combinations of processing steps in two contrasting ecosystems. Atmos. Meas. Tech. 9:4915-4933.

Mölder M et al. 2000. Water vapor, CO_2, and temperature profiles in and above a forest – accuracy assessment of an unattended measurement system. J. Atmos. Oceanic Technol. 17:417-425.

Oren R et al. 2006. Estimating the uncertainty in annual net ecosystem carbon exchange: spatial variation in turbulent fluxes and sampling errors in eddy-covariance measurements. Glob. Chang. Biol. 12:883-896.

Papale D et al. 2006. Towards a standardized processing of net ecosystem exchange measured with eddy covariance technique: algorithms and uncertainty estimation. Biogeosciences 3:571-583.

Rannik Ü et al., 2003. Turbulence statistics inside and over forest: influence on footprint prediction. Bound Layer Meteorol 109:163–189.

Rannik Ü et al. 2004. Estimation of forest-atmosphere CO_2 exchange by eddy covariance and profile techniques. Agr. Forest Meteorol. 126:141-155.

Rannik Ü et al., 2006. Uncertainties in measurement and modelling of net ecosystem exchange of a forest. Agr. Forest Meteorol. 138:244-257.

Schmid H et al. 2003. Ecosystem-atmosphere exchange of carbon dioxide over a mixed hardwood forest in Northern Lower Michigan. J. Geophys. Res. Atmos. 108(D14): Art. No. 4417.

Wesely M, Hart R, 1985. Variability of short term eddy correlation estimates of mass exchange. In: Hutchinson B, Hicks B (eds) The forest-atmosphere interaction. D. Reidel, Dordrecht, pp 591-612.

Wilson J, Swaters G, 1991. The source area influencing a measurement in the planetary boundary-layer – the footprint and the distribution of contact distance. Bound Layer Meteorol 55:25-46.